

Streamlined Genome Engineering with a Self-Excising Drug Selection Cassette

Daniel J. Dickinson,¹ Ariel M. Pani, Jennifer K. Heppert, Christopher D. Higgins, and Bob Goldstein

Department of Biology and Lineberger Comprehensive Cancer Center, University of North Carolina, Chapel Hill, North Carolina 27599-3280

ABSTRACT A central goal in the development of genome engineering technology is to reduce the time and labor required to produce custom genome modifications. Here we describe a new selection strategy for producing fluorescent protein (FP) knock-ins using CRISPR/Cas9-triggered homologous recombination. We have tested our approach in *Caenorhabditis elegans*. This approach has been designed to minimize hands-on labor at each step of the procedure. Central to our strategy is a newly developed self-excising cassette (SEC) for drug selection. SEC consists of three parts: a drug-resistance gene, a visible phenotypic marker, and an inducible Cre recombinase. SEC is flanked by *LoxP* sites and placed within a synthetic intron of a fluorescent protein tag, resulting in an FP-SEC module that can be inserted into any *C. elegans* gene. Upon heat shock, SEC excises itself from the genome, leaving no exogenous sequences outside the fluorescent protein tag. With our approach, one can generate knock-in alleles in any genetic background, with no PCR screening required and without the need for a second injection step to remove the selectable marker. Moreover, this strategy makes it possible to produce a fluorescent protein fusion, a transcriptional reporter and a strong loss-of-function allele for any gene of interest in a single injection step.

KEYWORDS CRISPR/Cas9; homologous recombination; gene tagging; *Caenorhabditis elegans*; self-excising cassette

A common goal in biological and biomedical research is to visualize the localization of a protein of interest within a cell or organism. This is often accomplished by fusing GFP or another fluorescent protein (FP) to the protein of interest. In the nematode *Caenorhabditis elegans*, GFP fusions were historically generated by injecting plasmids into the gonad of the adult hermaphrodite worm, resulting in the formation of extrachromosomal arrays (Mello *et al.* 1991). However, the resulting fusion proteins were typically strongly overexpressed in somatic tissues and silenced in the germline. Microparticle bombardment allowed the generation of low-copy transgenes that in some cases more closely recapitulated endogenous expression levels (Praitis *et al.* 2001; Sarov *et al.* 2012), but this technique is inefficient, time consuming, and difficult and requires expensive equipment and materials. More recently, we and others have re-

ported CRISPR/Cas9-based approaches that together can be used to make essentially any desired change to the *C. elegans* genome, including insertion of GFP into endogenous loci (Friedland *et al.* 2013; Dickinson *et al.* 2013; Lo *et al.* 2013; Chiu *et al.* 2013; Cho *et al.* 2013; Katic and Großhans 2013; Tzur *et al.* 2013; Waaijers *et al.* 2013; Chen *et al.* 2013; Zhao *et al.* 2014; Kim *et al.* 2014; Arribere *et al.* 2014; Paix *et al.* 2014; Ward 2015; Farboud and Meyer 2015). The resulting GFP knock-in strains express 100% labeled protein under the control of all native regulatory elements, resulting in endogenous levels and patterns of expression in all cases reported to date (Dickinson *et al.* 2013; Kim *et al.* 2014).

Our published approach for generating GFP knock-ins (Dickinson *et al.* 2013) made use of a selection strategy that was originally developed for single-copy transgene construction (Frøkjær-Jensen *et al.* 2008, 2012). This strategy is based on rescue of an *unc-119* mutant phenotype. *unc-119(ed3)* animals are nearly paralyzed, and when a functional copy of *unc-119* is integrated into the genome along with GFP or another modification, knock-in animals are easily identified by their wild-type movement. Although this strategy is extremely robust, it suffers from several important limitations. First, knock-ins must be generated in an

Copyright © 2015 by the Genetics Society of America

doi: 10.1534/genetics.115.178335

Manuscript received May 18, 2015; accepted for publication June 1, 2015; published Early Online June 3, 2015.

Supporting information is available online at <http://www.genetics.org/lookup/suppl/doi:10.1534/genetics.115.178335/-DC1>.

¹Corresponding author: 616 Fordham Hall, CB3280, Chapel Hill, NC 27599.

E-mail: ddickins@live.unc.edu

unc-119 mutant background. *unc-119* mutant animals are sick, difficult to inject, and likely carry additional undesired background mutations besides the mutation in *unc-119*. Second, the *unc-119* rescue strategy requires integration of *unc-119(+)* into the genome along with the desired genome modification. *unc-119(+)* can be flanked by *LoxP* sites, allowing it to be removed from the genome after knock-in isolation by injecting a plasmid encoding Cre recombinase (Dickinson *et al.* 2013); however, this requires an extra injection step, followed by outcrossing to remove the *unc-119(ed3)* mutant allele and still leaves behind a 34-bp *LoxP* scar. Finally, our published approach required construction of a complex homologous repair template plasmid for each new knock-in, which represents a significant investment of time and materials. These limitations have motivated other groups to develop alternative screening strategies that do not involve inserting a selectable marker along with the desired modification (Kim *et al.* 2014; Arribere *et al.* 2014; Paix *et al.* 2014; Ward 2015). Although valuable, these alternative strategies rely on PCR screening to identify knock-in animals, which is much more labor intensive than *unc-119* selection. In addition, selectable markers allow one to interrogate all progeny of injected animals (~10,000 in a typical experiment), whereas it is impractical to screen more than a few hundred animals by PCR. As a result, selection-based strategies are less sensitive to the choice of sgRNA and can more robustly identify genome editing events that occur at low frequency.

Here, we present a novel selection strategy especially tailored for inserting fluorescent proteins into the genome of *C. elegans*. Our approach does not require PCR screening or a second injection step; it inserts fluorescent proteins into the genome cleanly, leaving no exogenous sequences outside the fluorescent protein tag; and it can be used in wild-type animals and in most other genetic backgrounds. Moreover, this strategy can be used to produce a fluorescent protein fusion, a transcriptional reporter, and a strong loss-of-function allele for any gene of interest in a single injection step. Central to our approach is a new self-excising drug selection cassette that affords the benefits of positive selection without the limitations associated with *unc-119* selection. The total amount of hands-on labor required to tag a new gene is less than 1 day, which makes our new protocol the least labor-intensive approach reported to date for construction of new fluorescent protein fusions in *C. elegans*, to our knowledge.

Materials and Methods

Availability of protocols and reagents

A complete protocol for gene tagging using the self-excising cassette (SEC) is included in the Supporting Information. A continuously updated version will also be available on our website (<http://wormcas9hr.weebly.com>). FP-SEC vectors carrying worm codon-optimized GFP, the yellow FP YPET

and the red FPs mKate2 and TagRFP-T will be deposited at Addgene. The mNeonGreen (mNG) vector is available from the authors upon completion of a license agreement.

Strains and culture conditions

Supporting Information, Table S1 lists the strains constructed for this study. Bristol N2 was used as wild type and is the parent strain of all new strains reported here. Worms were raised on standard NGM plates, fed *Escherichia coli* OP50, and kept at 20° except where otherwise noted.

Gene tagging using SEC

To generate knock-in strains using long homology arms, we followed exactly the protocol presented in the Supporting Information. In brief, 500–700 bp homology arms for each target were PCR amplified from N2 genomic DNA and inserted into the mNG[^]SEC[^]3xFlag vector pDD268 using Gibson assembly (New England BioLabs) (throughout this article, we use the [^] symbol to denote a synthetic intron-containing a *LoxP* site). The complete sequences of all repair templates used in this study are available upon request. Cas9 target sites were chosen using the MIT CRISPR design tool (<http://crispr.mit.edu>) and inserted into the Cas9–sgRNA vector pDD162 as previously described (Dickinson *et al.* 2013). Table S2 lists the sgRNA sequences used in this study. For each tagging experiment, a mixture of 50 ng/μl Cas9–sgRNA plasmid, 10 ng/μl repair template, and red fluorescent co-injection markers (Frøkjær-Jensen *et al.* 2008; Dickinson *et al.* 2013) was injected into the gonads of young adults. Injected animals were transferred to new OP50 plates (three animals per plate) and allowed to lay eggs for 2–3 days at 25° in the absence of selection. Then, hygromycin was added to a final concentration of 250 μg/ml and the plates were returned to 25° for an additional 3–4 days. Candidate knock-in animals (those that survived hygromycin selection, were Rollers (Rol) and lacked the red fluorescent extrachromosomal array markers) were singled to establish lines. Only one line from each injection plate was kept.

To generate knock-in strains using short homology arms, we designed primers to amplify mNG[^]SEC[^]3xFlag and add 35–40 bp homology arms, following the recommendations in Paix *et al.* (2014). PCR products were purified using a MinElute spin column (Qiagen) and injected at 50 ng/μl, along with a Cas9–sgRNA plasmid and red fluorescent co-injection markers.

To excise SEC, L1/L2 larvae from insertion strains were heat shocked for 4–5 hr at 32°, then placed at 20° for 5–7 days. Wild-type F1 progeny of the heat-shocked animals were singled to establish marker-excised strains. Initial insertion strains for *ebp-2*, *his-72*, *oma-2*, and *rap-1* were homozygous viable and segregated 100% Rol progeny prior to heat shock. Therefore, wild-type animals picked after heat shocking these strains had lost both copies of SEC. *gex-3*, *mex-5*, and *nmy-2* are essential genes (Guo and Kemphues 1996; Schubert *et al.* 2000; Soto *et al.* 2002) and so insertions at these loci were isolated and maintained as heterozygotes. The

resulting animals segregated ~1/4 wild-type progeny at each generation, so a wild-type phenotype alone was not a reliable indicator of SEC loss. For $mNG^{\wedge}SEC^{\wedge}3xFlag::mex-5$ and 6/9 $mNG^{\wedge}SEC^{\wedge}3xFlag::nmy-2$ strains, mNG fluorescence was easily visible on a dissecting microscope; therefore, to excise SEC from these strains, heterozygous insertion strains were heat shocked, and wild-type animals that had excised SEC were identified by mNG fluorescence. Some of these worms segregated 100% mNG-positive progeny, indicating homozygosity for the marker-excised alleles. For $mNG^{\wedge}SEC^{\wedge}3xFlag::gex-3$, which is located on chromosome IV, fluorescence was too dim to see by eye. Therefore, to excise SEC from this strain, heterozygous insertion animals were first mated to males carrying the $nT1 [qls51]$ (IV;V) balancer chromosome. The resulting $mNG^{\wedge}SEC^{\wedge}3xFlag::gex-3$ IV/ $nT1 [qls51]$ (IV;V) animals segregated 100% Rol progeny, as expected (because $nT1 [qls51]$ (IV;V) is homozygous lethal). These animals were heat shocked, and wild-type progeny were picked to establish marker-excised lines. Marker-excised animals that had lost the $nT1 [qls51]$ balancer (that is, $mNG^{\wedge}3xFlag::gex-3$ homozygotes) were viable and fertile, indicating that $gex-3$ function was restored after SEC excision. A similar approach (using the $HT2 [bli-4(e937) let-?(q782) qls48]$ (I;III) balancer) was used to excise SEC from the 3/9 $mNG^{\wedge}SEC^{\wedge}3xFlag::nmy-2$ I strains that displayed fainter mNG fluorescence (we attribute the faint fluorescence in these strains to germline silencing (Lee *et al.* 2012; Shirayama *et al.* 2012; Leopold *et al.* 2015)).

Microscopy

Embryos were dissected in egg buffer, transferred to poly-L-lysine-coated coverslips using a mouth pipet, and gently flattened using 2.5% agar pads. Whole worms were mounted on 2.5% agar pads containing 10 mM sodium azide as a paralytic. Immunostaining was done using a tube fixation protocol (Finney and Ruvkun 1990). Mixed stage worms were washed in deionized water, resuspended in fixative (30 mM PIPES pH 7.4, 160 mM KCl, 40 mM NaCl, 20 mM EGTA, 10 mM spermidine, 50% methanol, 1% paraformaldehyde) and frozen in liquid nitrogen. Worms were frozen and thawed three times to crack the cuticle, then incubated for 1 hr at 4° with gentle mixing on a turning wheel. After washing twice with Tris/Triton (TT) buffer (100 mM Tris pH 7.4, 1% Triton X-100, 1 mM EGTA), the worms were incubated for 2 hr at 37° in TT containing 1% β -mercaptoethanol. Worms were next washed with borate buffer (BB; 50 mM H₂BO₃, 25 mM NaOH, 0.01% Triton X-100); incubated for 15 min at 37° in BB containing 10 mM dithiothreitol; washed with BB; incubated for 15 min at room temperature in BB containing 0.3% hydrogen peroxide; washed with BB; and finally washed with antibody buffer (PBS containing 1 mM EDTA, 0.5% Triton X-100, 1 mg/ml BSA and 0.03% sodium azide). The worms were blocked with 10% goat serum in antibody buffer and then stained with anti-Flag (Sigma) followed by Cy5-anti-mouse

(Jackson Laboratories). The stained specimens were mounted in Slowfade Diamond mounting medium with DAPI (Life Technologies).

$mNG::his-72$ animals (Figure 2B, Figure 3C, and Figure S1B) were imaged using a Zeiss LSM710 laser scanning confocal microscope equipped with a 40 \times , 1.2 NA water immersion objective. mNG was excited using the 514-nm line of an Argon ion laser and detected using emission filters for YFP. DAPI was excited with a 405-nm laser, and Cy5 was excited with a 633-nm laser; the DAPI and Cy5 signals were collected simultaneously. $mNG::ebp-2$ embryos (Figure 5) were imaged using a Nikon Ti-E microscope equipped with a 100 \times , 1.49 NA objective, a Yokogawa CSU-X1 spinning disk head, and a Hamamatsu C9100-13 camera operated in non-EM mode. mNG was excited with a 488-nm diode laser and detected using emission filters for GFP. $mNG::mex-5$ embryos (Figure 5) were imaged using the same Ti-E microscope, but using a 60 \times , 1.4 N objective, a 514-nm diode laser for excitation, and YFP emission filters for detection. $mNG::gex-3$ and $mNG::nmy-2$ worms and embryos (Figure 5) were imaged using a Nikon TE2000 microscope equipped with a 60 \times , 1.4 NA objective, a Yokogawa CSU-10 spinning disk head, and a Hamamatsu Orca ER camera. mNG was excited with a 514-nm diode laser and detected using emission filters for YFP. $mNG::rap-1$ worms (Figure 5) were imaged with the same TE2000 microscope but using a 20 \times , 0.5 NA objective. $mNG::oma-2$ worms (Figure 5) were imaged using a Nikon Eclipse Ti microscope equipped with epifluorescence illumination and a 20 \times , 0.5 NA objective. A FITC filter cube was used to excite and detect mNG.

To prepare figures for publication, images were cropped and rotated, brightness and contrast were adjusted, and maximum intensity projections (where applicable) were performed using FIJI. In addition, the “despeckle” function was applied to the $mNG::oma-2$ images to remove hot pixels that are a feature of the camera. No other image manipulations were performed.

RNA isolation and qRT-PCR

For RNA isolation, mixed stage worms were washed with M9 and dissolved in Trizol (Life Technologies). After addition of chloroform to separate phases, RNA was isolated from the upper aqueous phase using the RNeasy kit (Qiagen) according to the manufacturer’s instructions. Genomic DNA contamination was removed using an on-column DNase digestion kit (Qiagen). Poly(T)-primed cDNA was then prepared using the Superscript III reverse transcriptase kit (Life Technologies). qRT-PCR was performed using a Vii7 real-time PCR instrument and SYBR Green master mix (Life Technologies). Transcripts containing the $his-72$ ORF were detected with forward primer 5'-TCGTTTCGTGAGATTGCCAG-3' and reverse primer 5'-GAGTCCGACGAGGTATGCTT-3'. Y45F10D.4 was used for normalization (Hoogewijs *et al.* 2008; Zhang *et al.* 2012). The data were analyzed using Vii7 software, with the default settings for a relative standard curve experiment.

Genomic DNA isolation and PCR

Genomic DNA was isolated from the organic phase of Trizol extracts (see above) after phase separation, according to the manufacturer's instructions. For genotyping of the *his-72* locus (Figure 3B) we used forward primer 5'-GACCCCA CAAAATCGATACG-3' and reverse primer 5'-GAGTCCGAC GAGGTATGCTT-3'. Genotyping reactions were run using LongAmp Taq DNA polymerase (New England BioLabs). For qPCR of genomic DNA, we used the same instrument, reagents, and analysis settings as above. Marker-excised *mNG^{3xFlag}* was detected with forward primer 5'-GAGAATCTGTACTTTCAATCCGGA-3' and reverse primer 5'-TCTCTTGTATCGTCATCCT-3'. The *his-72* ORF, detected using the primers above, was used for normalization.

RNAi

Depletion of *hsf-1* was done by feeding using clone I-6C09 from the Ahringer library (Kamath and Ahringer 2003). We sequenced our clone to verify that the correct gene was targeted. Young adults that had not yet begun to produce embryos were placed on feeding plates, and their progeny were collected for imaging and qPCR when they reached adulthood (4 days later).

Results

Design of a new gene tagging strategy

Because of the limitations of our published *unc-119* selection approach (Dickinson *et al.* 2013) (see *Introduction*), we set out to develop a new selection approach for fluorescent protein tagging of endogenous genes via Cas9-triggered homologous recombination. Our goal was to minimize the hands-on labor required at every step of the procedure. We first sought a positive selectable marker that could be used in a wild-type background, as an alternative to *unc-119* selection that requires working in an *unc-119* mutant background. Hygromycin resistance has been reported to be an effective selectable marker in *C. elegans* (Greiss and Chin 2011; Radman *et al.* 2013; Chen *et al.* 2013). We confirmed that hygromycin killed 100% of nontransformed worms within 2–3 days, and a single heterozygous copy of the hygromycin phosphotransferase gene (*hygR*) was sufficient to confer resistance. Hygromycin selection can in principle be used in any genetic background, and it is also slightly faster than *unc-119* selection (6 days for hygromycin vs. 8–10 days for *unc-119*).

The only disadvantage of hygromycin selection compared to *unc-119* selection for knock-in experiments is that *hygR* does not confer a visible plate-level phenotype (in contrast, *unc-119(+)* worms are wild type, while their nontransformed siblings are Uncoordinated, *Unc*). Our published protocol (Dickinson *et al.* 2013) relied on the visible phenotype conferred by *unc-119(+)* at two stages: first, to identify animals that were homozygous for an insertion, and second, to identify animals that had excised the *unc-119(+)* marker

after Cre injection. We therefore sought a dominant marker that we could integrate along with *hygR* in order to confer a visible plate-level phenotype. We tested several classical dominant alleles and found that *sqt-1(e1350)* confers a strong and 100% penetrant *Rol* phenotype when expressed transgenically from a single-copy insertion (Figure 1B, left). We therefore included *sqt-1(e1350)* as a dominant phenotypic marker along with *hygR* within our selection cassette (Figure 1A). Compared to the more widely used *rol-6(su1006)*, *sqt-1(e1350)* had a stronger and more penetrant phenotype. Note that *sqt-1(e1350)* has also been used as a marker in “co-conversion” approaches (Arribere *et al.* 2014), but co-conversion of the endogenous *sqt-1* gene in that application differs from the use of transgenically expressed *sqt-1(d)* as a dominant marker here.

Next, we sought to eliminate the second injection step that was required to remove a *LoxP*-flanked selectable marker in our original protocol (Dickinson *et al.* 2013). We constructed a mini-gene (*hs::Cre*) composed of Cre recombinase under the control of the *hsp-16.41* heat-shock-inducible promoter and inserted it between the *sqt-1(d)* and *hygR* genes in our selection cassette (Figure 1A). The entire *sqt-1(d)::hsCre::hygR* construct is flanked by *LoxP* sites (Figure 1A). Thus, upon heat shock, expression of Cre recombinase should excise the selection cassette from the genome. We therefore refer to the selection cassette composed of *sqt-1(d)*, *hs::Cre*, and *hygR* as a self-excising cassette (SEC). In pilot experiments, we found that animals carrying SEC were 100% *Rol*, whereas after heat shock, wild-type animals appeared and were easy to distinguish from their *Rol* siblings (Figure 1B and File S2; see Figure 2C and Figure 4B, below, for measurements of self-excision efficiency).

Excision of a *LoxP*-flanked selectable marker from the genome leaves behind a 34-bp *LoxP* site. In principle, this residual *LoxP* site could interfere with gene regulation by, for example, disrupting a transcription factor binding site. To minimize the potential impact of the residual *LoxP* site, we placed SEC within a synthetic intron between the FP and 3xFlag sequences of an FP::3xFlag tag (Figure 1A, top). After SEC removal, the location of the residual *LoxP* site is within this synthetic intron (Figure 1A, bottom), where it is unlikely to interfere with gene regulation. This approach allows clean insertion of FP::3xFlag into the genome, with no exogenous sequences left outside the fluorescent protein tag.

Finally, we addressed the labor-intensive cloning step that was required in our previous *unc-119(+)*-based approach (Dickinson *et al.* 2013). Importantly, the inclusion of SEC within the FP tag generates a 1-piece FP[^]SEC[^]3xFlag module that can be inserted anywhere in the genome when appropriate homology arms are added. To facilitate addition of homology arms, we generated constructs in which the FP[^]SEC[^]3xFlag module is flanked by *ccdB* negative selection markers (Figure 1C, top). *ccdB* is toxic to *E. coli*, and *ccdB* negative selection is one of the key features that accounts for the high efficiency of Gateway cloning. In

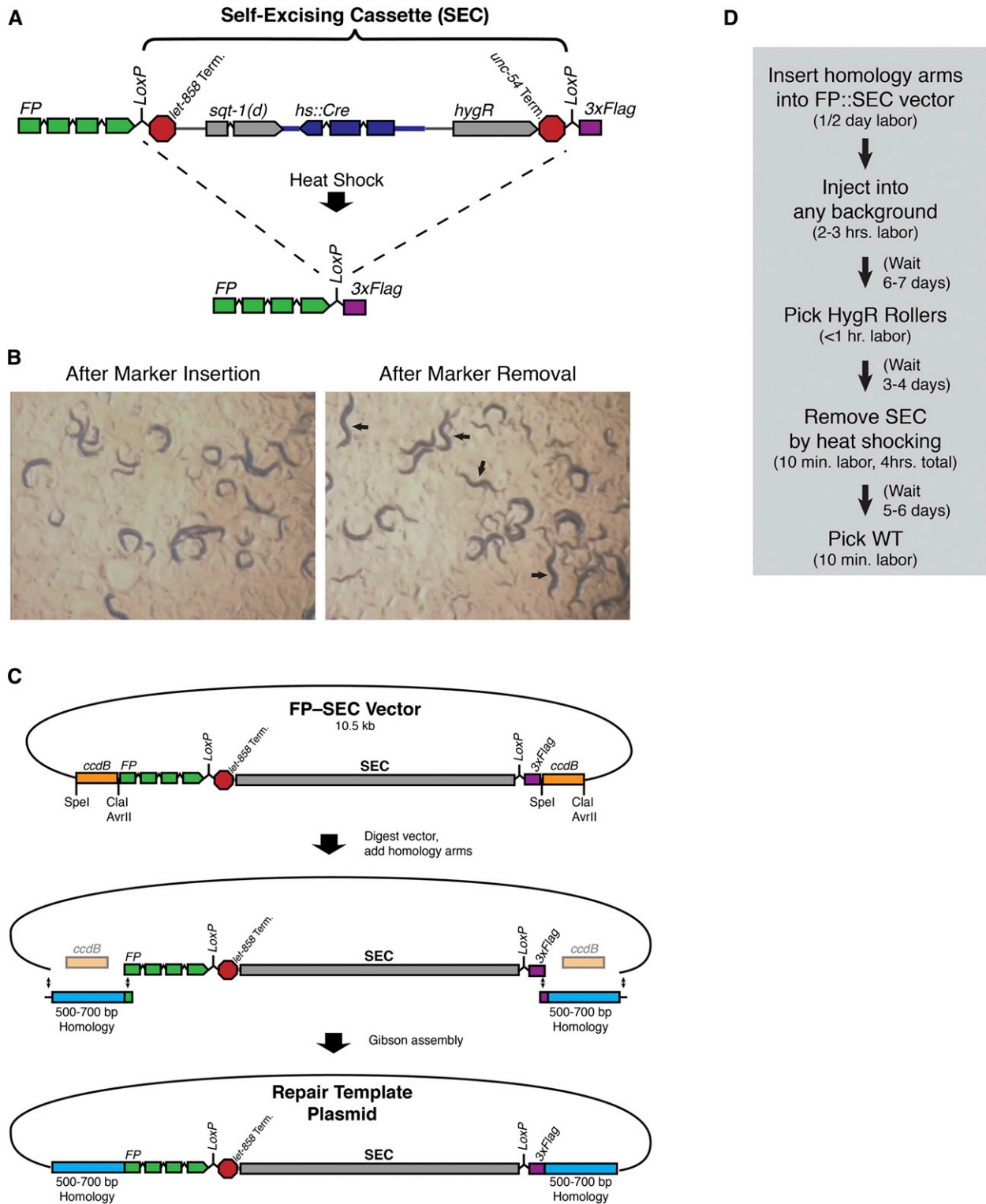


Figure 1 Design of an improved gene tagging workflow. (A) Design of a self-excising cassette for drug selection. SEC consists of a hygromycin resistance gene (*hygR*), a visible marker [*sqt-1(d)*], and an inducible Cre recombinase (*hs::Cre*). SEC is flanked by *LoxP* sites and placed within a synthetic intron in an FP::3xFlag tag, so that the *LoxP* site that remains after marker excision is within an intron. (B) Plate phenotype of animals homozygous for a *sqt-1(d)::hygR* selection marker (left) and appearance of wild-type animals after marker excision (right). Arrows indicate wild-type animals. See also File S2. (C) Schematic of an expedited cloning procedure for insertion of homology arms into an FP-SEC vector. The FP-SEC vector is first digested with restriction enzymes to release the *ccdB* markers, and 500–700 bp homology arms are inserted by Gibson assembly to generate the repair template plasmid. (D) Workflow for generation of new FP knock-ins using our strategy. The time required for each step is listed in parentheses.

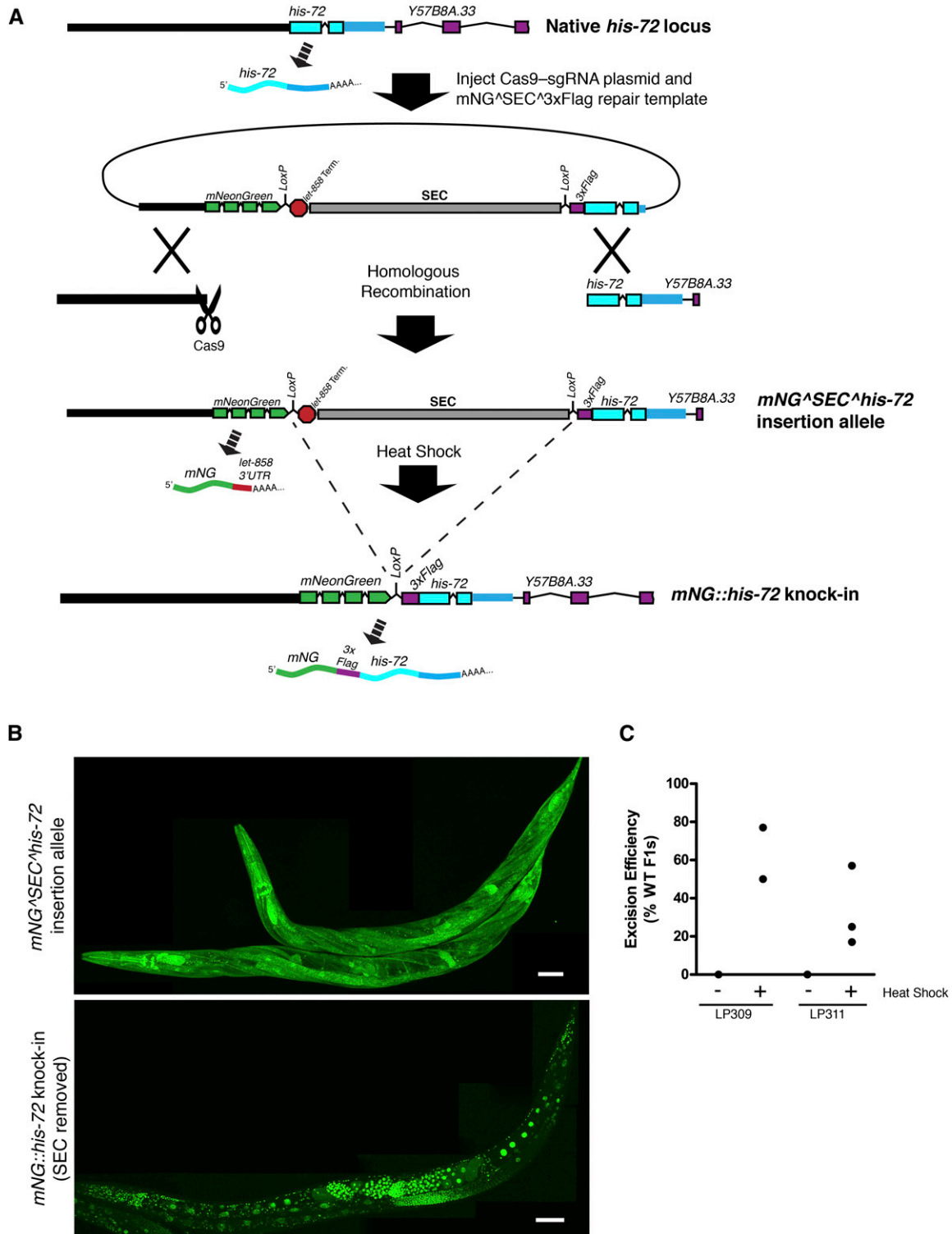


Figure 2 Tagging of *his-72* with mNG[^]3xFlag. (A) Illustration of the organization of the *his-72* locus and the predicted transcripts from this gene before editing (top), after homologous recombination (middle), and after SEC removal (bottom). (B) Images of adult mNG::his-72 worms before (strain LP309, top) and after (strain LP310, bottom) SEC removal. Shown are maximum intensity projections of a confocal Z series through entire worms. Scale bars, 50 μ m. (C) Efficiency of SEC excision following heat shock for two independent mNG[^]SEC[^]3xFlag::his-72 insertion strains. For each experiment, L1/L2 larvae were heat shocked, and the number of wild-type (WT) and Roller progeny were counted. Each data point represents an independent experiment in which all F1's present were counted ($n = 26$ –394 animals counted per experiment).

our constructs, each *ccdB* marker is flanked by unique restriction sites, which were chosen because they do not leave any residual sequence after digestion, allowing seamless fusion of FP[^]SEC[^]3xFlag to the homology arms. Homology arms can be cloned into these constructs using the following simple procedure (Figure 1C). First, the vector is digested with restriction enzymes to liberate the *ccdB* markers. Individual vector fragments are not purified; the entire digested vector is kept in one tube. A batch of digested vector may be stored and used to make multiple repair templates. Second, homology arms are PCR amplified using primers that add 20–30 bp of sequence overlapping the vector, to allow Gibson assembly. Third, the homology arms are mixed with the digested vector. The four repair template fragments (two homology arms plus the FP[^]SEC[^]3xFlag and backbone vector fragments) are joined together by Gibson assembly, and the resulting plasmids are transformed into competent *E. coli*. Since the parent vector (containing *ccdB* markers) does not transform, only clones that have correctly inserted both homology arms should grow. Therefore, correct clones can be identified by sequencing alone, without screening clones for inserts.

To test this cloning strategy, we generated 8 different homologous repair templates (targeting 8 different genes) in parallel, which took approximately half of a day. We directly sequenced 6 random clones of each of the 8 constructs (48 clones total). For 7/8 constructs, a total of >90% of clones (39 of 42 clones total) contained correctly inserted homology arms. For the eighth construct, one of the homology arm PCR products was obtained at low yield, and so the assembly was less efficient. This reaction still yielded a correct clone, although 12 clones had to be sequenced to identify one that was correct. We conclude that this cloning strategy allows robust insertion of homology arms into FP–SEC vectors with minimal labor.

With these technical and methodological innovations, our workflow for gene tagging consists of four steps (Figure 1D): (1) insertion of homology arms into an FP[^]SEC[^]3xFlag module; (2) injection; (3) picking Rollers that survive hygromycin selection; and (4) heat shocking to remove SEC. Importantly, the same workflow can be used to place FP::3xFlag at the N terminus, C terminus, or internally for any gene of interest, or to generate whole-gene deletions by replacing an entire coding region with FP[^]SEC[^]3xFlag. This workflow eliminates the most labor-intensive steps that were required in previous protocols (Dickinson *et al.* 2013; Paix *et al.* 2014).

Generation of a loss-of-function allele, promoter fusion, and protein fusion in a single injection step

As a first test of our approach, we inserted fluorescent protein at the N terminus of the *his-72* gene, which encodes a broadly expressed Histone H3.3 (Ooi *et al.* 2006). We chose to target the N terminus of *his-72* rather than the C terminus to take advantage of an additional feature of the FP[^]SEC[^]3xFlag design. We predicted that because SEC

contains transcriptional terminators, insertion of SEC at the 5' end of *his-72* should disrupt the gene by separating the promoter and coding region, resulting in a loss-of-function allele that expresses mNG in place of HIS-72 (Figure 2A). This allele should then convert to an N-terminal protein tag after SEC excision. Thus, N-terminal insertion of mNG[^]SEC[^]3xFlag into a gene of interest should produce a loss-of-function allele, a promoter fusion, and a protein fusion in a single injection step (Figure 2A).

We generated a homologous repair template for *mNG[^]SEC[^]3xFlag::his-72* using the procedure outlined in Figure 1C and injected it into the germlines of wild-type animals along with an appropriate Cas9–sgRNA plasmid. Our injection mix also contained mCherry markers that we used to distinguish extrachromosomal arrays from insertions, as has been done previously (Frøkjær-Jensen *et al.* 2008, 2012; Dickinson *et al.* 2013). From 72 injected animals, we obtained 9 independent strains carrying an insertion of mNG[^]SEC[^]3xFlag at the 5' end of *his-72*. Because *his-72* is nonessential (Ooi *et al.* 2006), we were able to readily isolate homozygous insertion strains by choosing animals that segregated 100% Rol progeny. These animals showed cytosolic mNG fluorescence in most tissues, consistent with the known expression pattern of *his-72* (Figure 2B, top).

Next, we heat shocked animals from these strains to remove SEC. After heat shocking L1/L2 animals, we readily identified wild-type animals in the F1 progeny of the heat-shocked animals for 9/9 strains. Strikingly, these animals exhibited strictly nuclear mNG fluorescence (Figure 2B), which is the expected pattern for a HIS-72 fusion protein (Ooi *et al.* 2006; Dickinson *et al.* 2013). These data indicate that N-terminal insertions of mNG[^]SEC[^]3xFlag behave as expected: the insertion allele expresses mNG from the gene's promoter, and an N-terminal protein fusion is produced after SEC removal by heat shock.

We quantified the frequency of SEC excision for two *mNG[^]SEC[^]3xFlag::his-72* strains. In five independent experiments, the F1 progeny of heat-shocked animals ranged from 17 to 77% wild type, with a mean of 45% (Figure 2C) (note that animals must excise both copies of SEC in order to display a wild-type phenotype in the F1). Although the frequency of excision varied between individual experiments, wild-type animals that had excised SEC were easily identified even on the plates that showed the lowest excision frequency. These results indicate that SEC excision by heat shock is highly efficient. By picking wild-type animals to new plates, we established strains with *mNG[^]3xFlag* fused cleanly to *his-72*. For clarity, we refer to mNG[^]SEC[^]3xFlag knock-in strains (prior to heat shock) as “initial insertion” strains, and mNG[^]3xFlag protein fusion strains (after heat shock) as “marker-excised” strains.

Spontaneous SEC excision can occur in certain tissues

We sought to test more quantitatively our prediction that expression of a gene of interest should be abolished upon N-terminal SEC insertion and restored following SEC excision.

To do this, we measured the expression of the *his-72* ORF in two pairs of strains before and after SEC removal (strains LP310 and LP312 are marker-excised derivatives of LP309 and LP311, respectively). As expected, *his-72* expression was strongly reduced in the mNG⁺SEC⁺3xFlag insertion strains, and expression was restored to wild-type levels after SEC removal (Figure 3A). However, we were surprised to find that *his-72* was still expressed at detectable levels (~15% of wild type) in the initial insertion strains. The reason for this became clear when we genotyped these strains with PCR primers that flank the insertion site. As expected, we detected a 1.5-kb band in N2 lysates, corresponding to the unmodified locus; an 8 kb band in initial insertion strains, indicating correct single-copy insertion of mNG⁺SEC⁺3xFlag; and a 2.5-kb band in marker-excised strains following SEC removal (Figure 3B). However, we also observed the 2.5-kb band, indicating excision of SEC, in the initial insertion strains that had not been heat shocked (Figure 3B, lanes 2 and 4). These data indicate that either a fraction of worms in each sample, or a fraction of cells within each worm, spontaneously excised SEC in the absence of heat shock. We were able to rule out the former possibility because the initial insertion strains continued to produce 100% Rol progeny over multiple generations. We therefore inferred that some cells in each worm spontaneously excise SEC in the absence of heat shock.

To estimate the prevalence of spontaneous self-excision, we performed qPCR on genomic DNA samples. We used primers flanking the *LoxP*-containing intron left behind after SEC excision, which amplified a single product corresponding to marker-excised mNG⁺3xFlag. The abundance of mNG⁺3xFlag in each sample is a measure of the fraction of haploid genomes in that sample that have undergone SEC excision. Using qPCR, we determined that the initial insertion strains LP309 and LP311 had 2.5 and 2.3% as much genomic mNG⁺3xFlag, respectively, as their marker-excised derivatives LP310 and LP312. These data suggest that spontaneous self-excision occurs in a relatively small fraction of cells.

To identify the cells that spontaneously excise SEC, we stained whole worms with anti-Flag antibodies. Because the 3xFlag tag is located downstream of SEC and does not carry its own start codon, only cells that have excised SEC should be stained. As a control, anti-Flag staining was detected in all, or almost all, nuclei in marker-excised animals (Figure 3C, bottom). In the initial insertion strains, reproducible anti-Flag staining was observed in the nuclei of the intestine and in a small number of nuclei in the head and tail (Figure 3C, top). Intestinal anti-Flag staining was observed in every animal examined, while the staining in head and tail nuclei was fainter and more variable. The stained nuclei in the head and tail were concentrated in the nerve ring between the two pharyngeal bulbs and postanally in a bilaterally symmetric pattern in the tail, respectively, suggesting that these cells are likely to be neurons. Consistent with a tendency for neurons to spontaneously excise SEC, we also saw stained cells in the ventral nerve cord in a minority of

specimens (D.J.D., unpublished results). Additionally, in a minority of specimens we observed nuclear staining in cells in the center of the animal, near the developing vulva (Figure 3C, asterisk), but this staining may be nonspecific as it was also observed in one N2 animal.

Because Cre recombinase is under the control of a heat shock promoter in our strains, we tested whether spontaneous self-excision required a functional heat-shock response. Treatment of animals with RNAi against *hsf-1*, which is known to be required for the transcriptional response to heat shock (Hajdu-Cronin *et al.* 2004), did not prevent intestinal nuclei from spontaneously excising SEC (Figure S1). To verify the effectiveness of RNAi, we heat shocked L1/L2 larvae from control or *hsf-1* RNAi plates. Control animals produced abundant wild-type progeny after heat shock, but *hsf-1* RNAi animals produced 100% Rol progeny, indicating that *hsf-1* RNAi prevented heat-shock-induced activation of Cre recombinase. Growth of worms at 15° also had little to no effect on expression levels of the *his-72* ORF in initial insertion strains (Figure S1), suggesting that SEC excision in intestinal cells is not due to low-level heat stress in worms maintained at 20° or 25°. Spontaneous SEC excision may therefore reflect a normal physiological activation of the *hsp-16.41* promoter during intestinal development. In summary, these data are consistent with our prediction that N-terminal insertions of FP⁺SEC⁺3xFlag behave as strong loss-of-function alleles, with the caveat that spontaneous self-excision—resulting in expression of the protein of interest—can occur in the absence of heat shock in the intestine and in certain neurons.

SEC selection is robust across a wide range of loci

Having established that our tagging strategy performed as designed for the *his-72* locus, we next tested whether it would be generally applicable to a wider range of genes. First, we sought to quantitatively compare the efficiency of SEC selection to *unc-119(+)* selection. To do this, we generated a derivative of the MosSCI targeting vector pCFJ150 (Frøkjær-Jensen *et al.* 2008) that carried SEC in place of *unc-119(+)*. We previously showed that Cas9 could be used in place of Mos1 to generate the DNA double-strand break that allows insertion of transgenes cloned into pCFJ150 at the *ttTi5605* locus on chromosome II (Dickinson *et al.* 2013). We compared the efficiency of Cas9-mediated transgene insertion using either *unc-119(+)* or SEC selection. Although the insertion frequency varied between individual experiments, as previously reported (Dickinson *et al.* 2013), overall the efficiency of SEC selection was indistinguishable from *unc-119(+)* (Figure 4A). To ensure that the ability to excise SEC following heat shock was not specific to any one locus, we selected two transgenic strains from this experiment and measured the frequency of SEC excision following heat shock. Similar to our observations at the *his-72* locus (Figure 2C), SEC excision frequency at the *ttTi5605* locus varied from plate to plate but was always high enough that it was easy to identify marker-excised animals (Figure 4B).

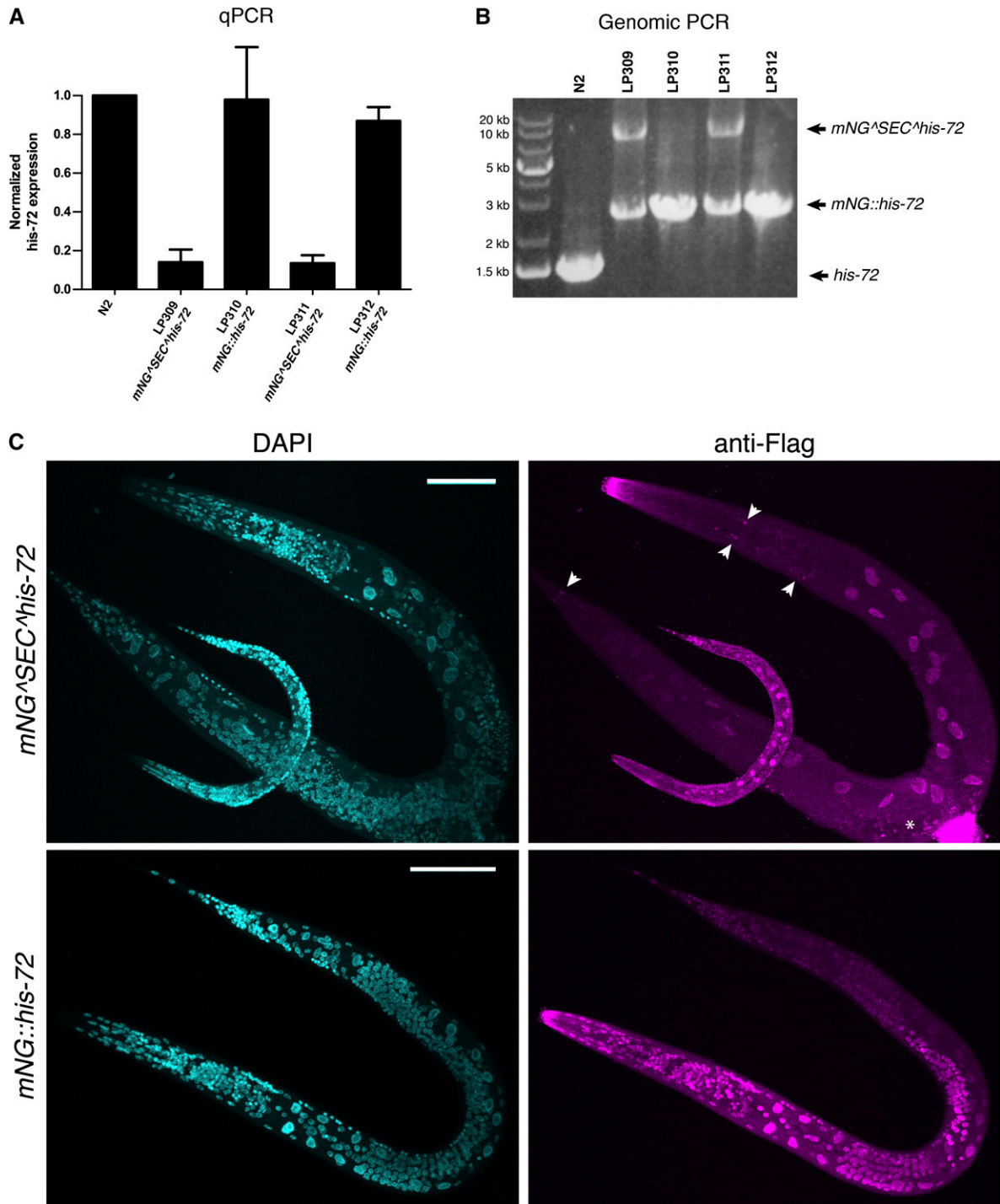


Figure 3 *his-72* expression levels and spontaneous loss of SEC from a subset of cells. (A) Expression of the *his-72* ORF measured by qPCR in wild-type (N2), initial insertion (LP309 and LP311), and marker excised (LP310 and LP312) strains. Results are the means of three independent experiments, and error bars indicate 95% confidence intervals. (B) Genotyping of the strains in A. The lower band in LP309 and LP311 indicates spontaneous self-excision of SEC in a population of cells in the absence of heat shock. (C) Images of L4 worms of the indicated genotypes stained with anti-Flag antibodies to label cells that have excised SEC (spontaneously in the *mNG[^]SEC[^]his-72* strain LP309, or after heat shock in the *mNG[^]::his-72* strain LP310). Shown are maximum intensity projections of a confocal Z series through entire worms. Scale bars, 50 μ m. Arrowheads indicate stained cells in the head and tail, and the asterisk indicates staining near the developing vulva that may be nonspecific (see text for details).

Next, we designed and cloned homologous repair templates to generate N-terminal *mNG[^]3xFlag* tags on seven additional genes. We injected 60–78 animals per construct

and obtained *mNG[^]SEC[^]3xFlag* insertions on the first attempt for six of seven targets, five of which yielded multiple independent lines (Figure 4C and Table 1). Plasmid

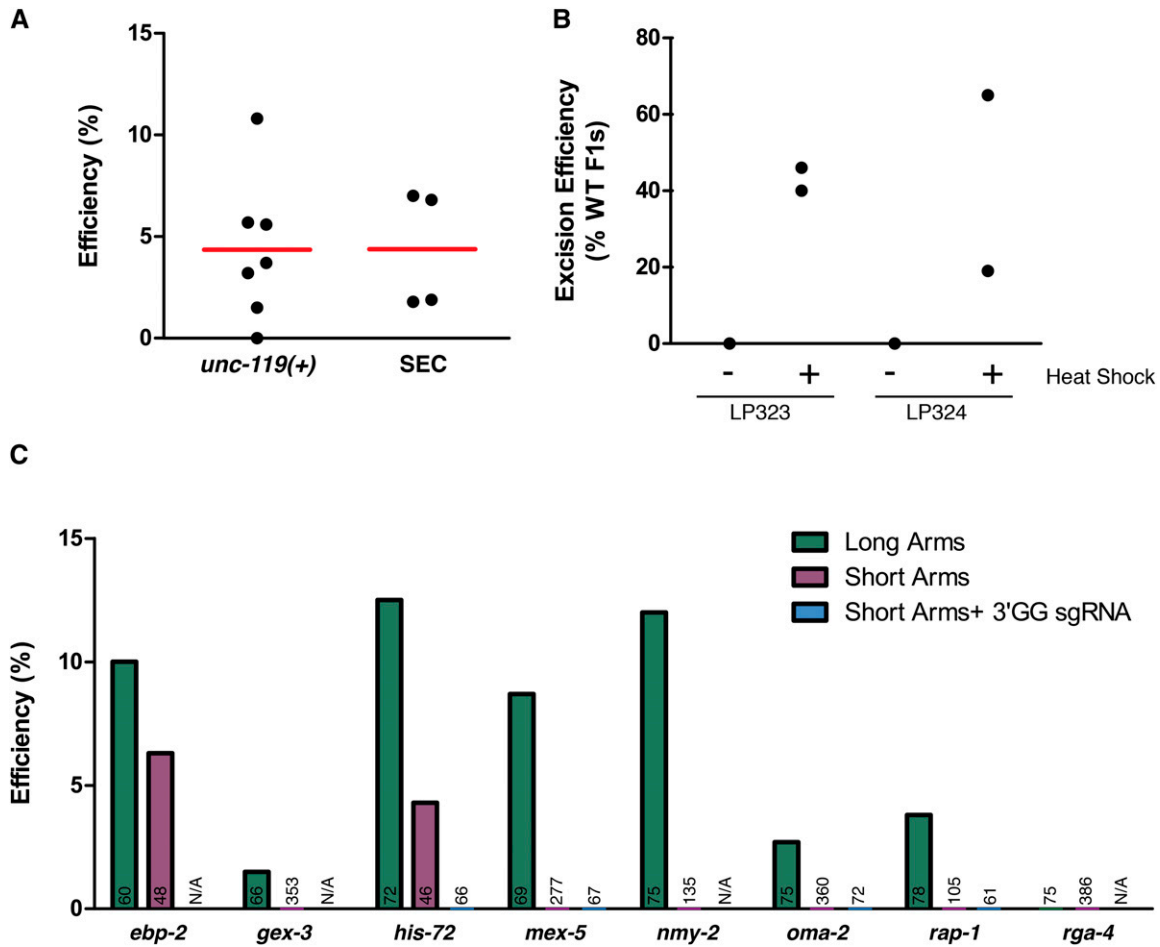


Figure 4 Efficiency of genome engineering using SEC. (A) Comparison of single-copy transgene insertion at the *ttTi5605* locus using either *unc-119(+)* or SEC selection. Each data point represents a single experiment, and red lines show the means across experiments; 45–90 animals were injected for each experiment. Efficiency is defined as the fraction of injected animals yielding insertions. (B) Efficiency of SEC excision following heat shock, measured as in Figure 2C, for two transgenes at the *ttTi5605* locus. Each data point represents an independent experiment in which all F1's present were counted ($n = 299$ – 913 animals counted per experiment). (C) Efficiency of precise mNG^{SEC}3xFlag insertion into eight different endogenous loci using long homology arms (500–700 bp; green bars), short homology arms (35–40 bp; purple bars) or short homology arms and 3'GG sgRNAs (blue bars). Numbers on each bar indicate the number of animals injected, and efficiency is defined as the fraction of injected animals yielding precise insertions. N/A, not applicable (3'GG sgRNAs were tested only for the genes where a 3'GG target was present near the site of insertion). See also Table 1.

construction and injections for these genes were done in parallel, requiring a total of ~4 days of hands-on labor for all seven targets (~1/2 day total per target), including all cloning steps. Of the strains generated in these experiments, 91% (32/35) yielded marker-excised derivatives following heat shock. Interestingly, a few strains (6/35) spontaneously excised SEC in the germline and produced marker-excised progeny without needing to be heat shocked. These events were sufficiently rare that they did not undermine the efficacy of SEC selection, nor did they prevent us from using the *Rol* phenotype to derive or maintain homozygous insertion lines. Overall, these results demonstrate that our procedure is robust and efficient and can be used to tag a wide range of *C. elegans* genes.

In *C. elegans* and other systems, Cas9 cleavage efficiency can vary substantially depending on the choice of sgRNA (Friedland *et al.* 2013; Waaijers *et al.* 2013; Shalem *et al.*

2014; Wang *et al.* 2014; Kim *et al.* 2014; Doench *et al.* 2014; Farhoud and Meyer 2015), and sgRNA efficiency has been widely considered to be an important factor for the success of genome editing experiments in *C. elegans* (Kim *et al.* 2014; Arribere *et al.* 2014; Paix *et al.* 2014; Farhoud and Meyer 2015). Interestingly, we designed our sgRNAs without regard to predicted efficiency and tested only a single sgRNA per target, and yet still obtained insertions on the first attempt at 7/8 loci, suggesting that high levels of Cas9 activity may not be a prerequisite for SEC-based homologous recombination. To explore further the relationship between sgRNA choice and recombination efficiency, we scored all of our sgRNAs using an activity prediction algorithm (Doench *et al.* 2014). This analysis revealed no statistically significant correlation between sgRNA score and recombination efficiency (Spearman's $r = 0.18$; $P = 0.6$; Figure S2 and Table 1). Although we would need to test many more targets to

Table 1 Efficiency of mNG[^]SEC[^]3xFlag insertion into 8 different endogenous loci

Target	Homology arms	sgRNA	Doench <i>et al.</i> sgRNA score	Distance to cut (bp)	No. injected	Precise insertions	Imprecise insertions	False positives	Efficiency (%)
<i>ebp-2</i>	Long	Non-3'GG	0.555	4	60	6	0	0	10.0
<i>ebp-2</i>	Short	Non-3'GG	0.555	4	48	3	0	2	6.3
<i>gex-3</i>	Long	Non-3'GG	0.039	19	66	1	0	0	1.5
<i>gex-3</i>	Short	Non-3'GG	0.039	19	353	0	0	1	0.0
<i>his-72</i>	Long	Non-3'GG	0.027	5	72	9	0	0	12.5
<i>his-72</i>	Short	Non-3'GG	0.027	5	46	2	0	0	4.3
<i>his-72</i>	Short	3'gg	0.281	40	66	0	2	0	0.0
<i>mex-5</i>	Long	Non-3'GG	0.208	25	69	6	0	0	8.7
<i>mex-5</i>	Short	Non-3'GG	0.208	25	277	0	2	4	0.0
<i>mex-5</i>	Short	3'gg	0.427	29	67	0	2	1	0.0
<i>nmy-2</i>	Long	Non-3'GG	0.382	6	75	9	0	0	12.0
<i>nmy-2</i>	Short	Non-3'GG	0.382	6	135	0	1	2	0.0
<i>oma-2</i>	Long	Non-3'GG	0.112	2	75	2	0	0	2.7
<i>oma-2</i>	Short	Non-3'GG	0.112	2	360	0	0	10	0.0
<i>oma-2</i>	Short	3'gg	0.392	26	72	0	1	3	0.0
<i>rap-1</i>	Long	Non-3'GG	0.136	23	78	3	0	0	3.8
<i>rap-1</i>	Short	Non-3'GG	0.136	23	105	0	1	3	0.0
<i>rap-1</i>	Short	3'gg	0.282	32	61	0	0	1	0.0
<i>rga-4</i>	Long	Non-3'GG	0.150	4	75	0	0	0	0.0
<i>rga-4</i>	Short	Non-3'GG	0.150	4	386	0	3	14	0.0

Precise insertions are the desired single-copy integration events confirmed by PCR and/or the correct pattern of mNG fluorescence. Imprecise insertions are insertion events at correct locus, but carry rearrangements within the insertion. False positives are animals that lacked the red fluorescent extrachromosomal array markers but did not carry insertions at the desired locus. Efficiency is defined as the fraction of injected animals yielding precise insertions. See also Figure 4C.

rule out a relationship between sgRNA activity and recombination efficiency, these data indicate that our selection strategy can yield knock-ins without the need for extensive sgRNA optimization.

Short homology arms can support insertion of mNG[^]SEC[^]3xFlag, but with lower efficiency

While our experiments were in progress, Paix *et al.* (2014) reported that short (30–70 bp) homology arms are in many cases sufficient to mediate precise repair of Cas9-induced double-strand breaks, supporting edits ranging in size from single base pairs to insertion of GFP. We reasoned that in principle, this finding could allow us to streamline our protocol even further, by entirely eliminating the need for homologous repair template cloning. To test this idea, we designed PCR primers to amplify mNG[^]SEC[^]3xFlag, adding 35–40 bp of homology for insertion at each of the 8 loci we targeted above. We repeated the injections, substituting the appropriate mNG[^]SEC[^]3xFlag PCR product (with short homology arms) for the homologous repair template plasmid (with long homology arms) in each case.

We confirmed the finding (Paix *et al.* 2014) that short homology arms are sufficient to mediate site-specific homologous recombination at several different loci (Figure 4C and Table 1). However, the efficiency and robustness of recombination with 35–40 bp homology arms were much lower

than with 500–700 bp arms. Using short homology arms, we observed correct insertion of mNG[^]SEC[^]3xFlag for only 2/8 targets (*his-72* and *ebp-2*). The remaining targets failed to yield precise knock-ins, despite hundreds of animals injected (Figure 4C and Table 1). In an attempt to improve the efficiency of recombination with short homology arms, we tested several different PCR purification kits, used PAGE-purified primers for PCR, and titrated the repair template concentration in the injection mix over a 100-fold range. However, none of these measures resulted in improved efficiency (D.J.D., unpublished results).

Besides low efficiency, we also encountered other challenges with the use of short homology arms to insert mNG[^]SEC[^]3xFlag into the genome. First, we observed a higher false-positive rate (that is, a larger proportion of animals that lacked extrachromosomal array markers but did not carry insertions) when injecting PCR products compared to plasmids. This may be due to the fact that PCR products were injected at a higher concentration (50 ng/ μ l; Paix *et al.* 2014) compared to plasmids (10 ng/ μ l; Dickinson *et al.* 2013). Second, even among strains that carried *bona fide* insertions at the desired locus, a high proportion (12/17) of the strains generated using short homology arms had rearrangements within the insertion (“Imprecise Insertions” in Table 1), whereas no rearrangements were observed in this study when long homology

arms were used (although other studies have shown that rearrangements can occur, at low frequency, when using long homology arms with various means of transgene insertion; Berezikov *et al.* 2004; Frøkjær-Jensen *et al.* 2008; Dickinson *et al.* 2013). The majority (11/12) of the rearranged strains generated using short homology arms failed to show detectable mNG fluorescence. Finally, we found that in practice, generating mNG[^]SEC[^]3xFlag PCR products with 35–40 bp homology arms often required a similar amount of effort compared to cloning 500–700 bp homology arms with our *ccdB*-based approach (Figure 1C), because amplification of mNG[^]SEC[^]3xFlag (~6.5 kb) with long primers was more difficult than amplification and insertion of 500–700 bp homology arms into an FP–SEC vector. We conclude that, in our hands, the enhanced efficiency and robustness conferred by longer homology arms justifies any extra effort spent cloning repair template constructs.

Our results using long homology arms suggested that a high-efficiency sgRNA is not necessary for homologous recombination. Nevertheless, we wondered whether higher-activity sgRNAs could improve the low efficiency we observed for mNG[^]SEC[^]3xFlag insertion using short homology arms. Farboud and Meyer (2015) recently reported that sgRNAs whose target sequences end in a GG dinucleotide (3'GG sgRNAs) support much higher levels of Cas9 activity. Therefore, we generated 3'GG sgRNAs for the four loci on our targets list for which it was possible to design a 3'GG sgRNA that would cleave within 30–40 bp of the desired insertion site, and we repeated the injections targeting these loci. We obtained a modestly higher frequency of insertions using a 3'GG sgRNA for some of the loci tested (2/4 loci), but 5/5 of the resulting insertions carried rearrangements (Table 1). Even when these imprecise insertion events are included in the total, 3'GG sgRNAs with short homology arms yielded a lower frequency of insertions than non-3'GG sgRNAs with long homology arms. We conclude that the use of 3'GG sgRNAs does not increase short homology arm insertion efficiency to the level seen with long homology arms and does not overcome the propensity of short homology arm inserts to rearrange.

mNG[^]SEC[^]3xFlag knock-in strains behave as expected

Finally, we characterized the knock-in strains that we generated using our new tagging strategy. Of the eight genes we tagged N terminally with mNG[^]SEC[^]3xFlag, three (*gex-3*, *mex-5*, and *nmy-2*) are essential genes (Guo and Kemphues 1996; Schubert *et al.* 2000; Soto *et al.* 2002). As expected, the initial insertion strains for these loci were viable and fertile only as heterozygotes. Homozygous mNG[^]SEC[^]3xFlag::*gex-3* and mNG[^]SEC[^]3xFlag::*mex-5* insertions were maternal-effect lethal, as are previously described loss-of-function mutations in these genes (Schubert *et al.* 2000; Soto *et al.* 2002). Animals homozygous for an mNG[^]SEC[^]3xFlag::*nmy-2* insertion survived to adulthood, likely due to perdurance of maternal protein, but were ster-

ile. In each of these cases, viability and fertility were fully restored upon SEC excision. These results support our conclusion that N-terminal insertion of FP[^]SEC[^]3xFlag generates a loss-of-function allele and that gene function is restored upon SEC removal.

We examined mNG localization in all of our strains. In every case, we observed localization of the marker-excised fusion proteins that was consistent with our prior knowledge of the tagged proteins (Figure 5, right). mNG::*EBP-2* localized prominently around centrosomes (Figure 5, arrowheads), especially during mitosis, similar to the localization of endogenous *EBP-2* revealed by immunostaining (Srayko *et al.* 2005). mNG::*GEX-3* localized to cell boundaries throughout embryogenesis (Figure 5) (Soto *et al.* 2002). mNG::*MEX-5* was concentrated in the anterior cytoplasm of polarized one-cell embryos and localized to punctate structures (P granules) in the cytoplasm of germline precursor cells (Figure 5, arrowheads), and its expression became confined to the posterior blastomeres in older embryos (Schubert *et al.* 2000; Tenlen *et al.* 2008). mNG::*NMY-2* was enriched at the anterior cell cortex and in the cleavage furrow in the one-cell embryo (Figure 5, arrowheads) (Munro *et al.* 2004). mNG::*OMA-2* localized in the cytoplasm, and its expression was restricted to oocytes and one-cell embryos (Figure 5, arrowheads) (Detwiler *et al.* 2001). The localization of *RAP-1* has not been previously reported, but we found that mNG::*RAP-1* localized to the plasma membrane in a wide range of tissues including neurons, intestine, and the germline (Figure 5), consistent with the fact that *RAP-1* is a Ras-family small GTPase with a stereotypical C-terminal membrane-targeting sequence. In each of these cases, the expression of mNG in the initial insertion strain broadly mimicked that of the protein fusion, but lacked subcellular localization and, in the cases of *MEX-5* and *OMA-2*, regulation of localized expression that is known to be mediated at the protein level (Detwiler *et al.* 2001; Tenlen *et al.* 2008). These observations are consistent with our prediction that the initial insertion alleles behave as transcriptional reporters and are converted into protein fusions after SEC excision.

Discussion

We have developed a gene-tagging strategy that, to our knowledge, is the least labor-intensive method currently available for insertion of fluorescent protein tags into the *C. elegans* genome. Central to our approach is a novel self-excising drug selection cassette (SEC) that enables robust selection in any genetic background without PCR screening, following insertion alleles based on plate phenotype, and marker excision without a second injection step. SEC-based homologous recombination is also relatively insensitive to the choice of sgRNA, which simplifies experimental design. We anticipate that this tool will greatly facilitate tagging of *C. elegans* proteins for cell biological assays. Indeed, given the low amount of hands-on labor required to tag a new gene, it may now be feasible to generate a collection of

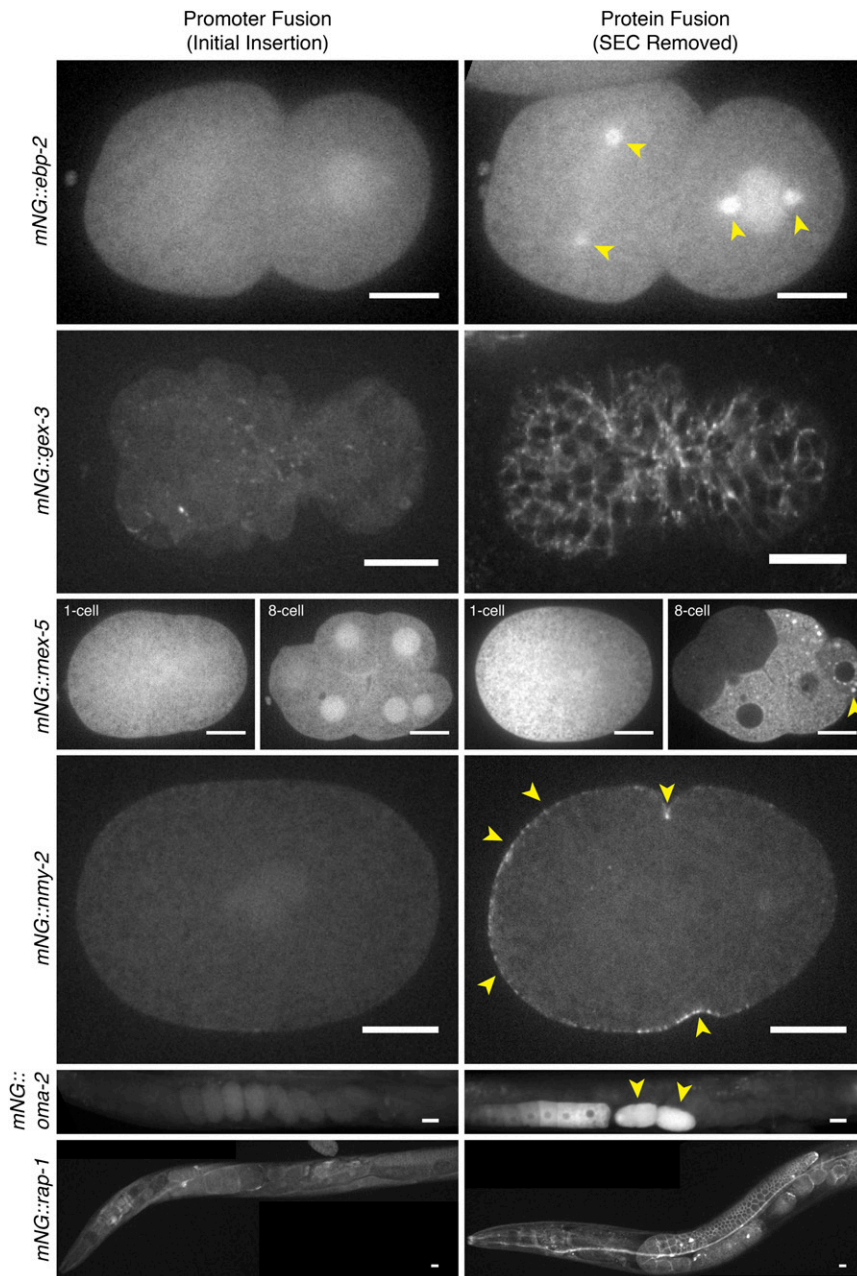


Figure 5 Images of knock-in strains generated using SEC. mNG fluorescence was imaged in the indicated strains. Left: initial insertions, which are predicted to behave as transcriptional reporters. Right: marker-excised strains, which express mNG^{3xFlag} fused to the protein of interest. The following strains are shown: *mNG^{SEC}3xFlag::ebp-2*, LP345; *mNG^{3xFlag}::ebp-2*, LP346; *mNG^{SEC}3xFlag::gex-3*, LP361; *mNG^{3xFlag}::gex-3*, LP362; *mNG^{SEC}3xFlag::mex-5*, LP366; *mNG^{3xFlag}::mex-5*, LP367; *mNG^{SEC}3xFlag::nmy-2*, LP388; *mNG^{3xFlag}::nmy-2*, LP389; *mNG^{SEC}3xFlag::oma-2*, LP390; *mNG^{3xFlag}::oma-2*, LP391; *mNG^{SEC}3xFlag::rap-1*, LP394; *mNG^{3xFlag}::rap-1*, LP395. Arrowheads indicate expected localization of the fusion proteins (see text for details). Scale bars, 10 μ m.

fluorescent protein knock-ins for every gene in the *C. elegans* genome. In addition, the ability to generate a loss-of-function mutation, transcriptional reporter, and tagged protein using a single workflow and injection step will simplify the initial characterization of unstudied or little-studied genes. Although we focused here on gene tagging, we anticipate that SEC will also facilitate the construction of other kinds of genome modifications.

For this study, we exclusively generated N-terminal mNG^{SEC}3xFlag knock-ins, because we wanted a large panel of N-terminal mNG^{SEC}3xFlag insertions in order to test our predictions about their behavior. However, it is important to emphasize that our workflow does not require placing a tag at the N terminus of a protein of interest. By

choosing an appropriate sgRNA and homology arms, it is feasible to insert FP^{SEC}3xFlag at any location in the genome, including at the C terminus, internally, or in place of any gene of interest. A C-terminal insertion of FP^{SEC}3xFlag generates a protein fusion immediately, but with the *let-858* 3'UTR that is part of SEC in place of the endogenous 3'UTR; the native 3'UTR is restored upon SEC excision (A.M.P and J.K.H., unpublished results). In addition, it should be possible to use SEC to produce other modifications besides simple FP insertions. For example, by cloning mutant sequences into FP-SEC vectors along with the homology arms, one could in principle tag a protein and at the same time introduce targeted mutations. More generally, we anticipate that SEC can be used in place of

unc-119(+) for any application that relies on a selectable marker.

One potential limitation of SEC is the tendency for the marker to spontaneously self-excise in the absence of heat shock. Spontaneous self-excision occurs in a fraction of cells in each worm, particularly in the intestine, and also occurs on rare occasions in the germline leading to permanent loss of SEC in an animal's progeny. This phenomenon does not affect the utility of SEC for gene tagging or other applications that involve positive selection, but it does prevent N-terminal FP[^]SEC[^]3xFlag insertions from being treated as true null alleles. Spontaneous self-excision is almost certainly due to low-level expression of Cre recombinase in the absence of heat shock. Therefore, it might be possible to prevent spontaneous self-excision by treating animals with RNAi against Cre. However, given the small amount of time and labor involved, deleting the entire coding region of a gene of interest and replacing it with FP[^]SEC[^]3xFlag might be a better strategy if a true null allele is required.

In the course of our experiments, we performed a direct comparison of homologous recombination efficiency mediated by short (35–40 bp) vs. long (500–700 bp) homology arms. Although we confirmed the finding that short homology arms can mediate homologous recombination (Paix *et al.* 2014), we found substantially higher efficiencies using longer arms. One important difference between our study and that of Paix *et al.* (2014) is the size of the DNA insertions we generated: the largest sequence inserted by Paix *et al.* was GFP, which is ~1 kb in size, whereas mNG[^]SEC[^]3xFlag is ~6.5 kb. Thus, our results may simply reflect a limit to the size of insertion that can be made using short homology arms. We also found that short homology arms yielded a much higher frequency of rearranged insertions. This result might not reflect a property of short homology arms *per se*, but instead may be due to the fact that our short homology arm repair templates were PCR products, while the long homology arm repair templates were plasmids. We suspect that linear DNA repair templates might be more prone to rearrangements because of their free ends. Although the need to clone longer homology arms might at first be viewed as a disadvantage of the SEC-based strategy, we emphasize that in our experience, the amount of labor required to clone homology arms using our expedited cloning strategy was very similar to that required to generate PCR repair templates using primers that include the homology arms. Moreover, any added effort spent cloning homology arms into an FP–SEC construct is made up for by higher recombination efficiency (Figure 4C) and by elimination of labor-intensive single worm PCR screening steps that are required for other protocols (Kim *et al.* 2014; Arribere *et al.* 2014; Paix *et al.* 2014; Ward 2015).

Finally, we note that, although we have demonstrated the utility of SEC for gene tagging in *C. elegans*, the design principles behind a self-excising selection cassette are not specific to this organism. The use of drug selection, which does not require preexisting mutations, should allow

straightforward extension of this approach to nonmodel nematodes, tissue culture cells, and possibly other invertebrates. Although the *sqt-1(d)* phenotypic marker is worm specific, it could easily be replaced by GFP or another marker. Finally, the placement of SEC within a synthetic intron of an FP::epitope tag should be applicable to any system where splicing rules are sufficiently well understood. Thus, our strategy may facilitate seamless insertion of fluorescent proteins via genome editing in a variety of organisms.

Acknowledgments

We thank Amy Maddox, David Reiner, Geraldine Seydoux, Jordan Ward, and members of the Goldstein lab for helpful discussions and comments on the manuscript. Some strains were provided by the *Caenorhabditis* Genetics Center, which is funded by the U.S. National Institutes of Health (NIH) Office of Research Infrastructure Programs (P40 OD010440). This work was supported by NIH T32 CA009156 (D.J.D. and A.M.P.); a Howard Hughes postdoctoral fellowship from the Helen Hay Whitney Foundation (D.J.D.); a U.S. National Science Foundation (NSF) graduate research fellowship (J.K.H.); and NIH R01 GM083071 and NSF IOS 0917726 (B.G.).

Literature Cited

- Arribere, J. A., R. T. Bell, B. X. H. Fu, K. L. Artilles, P. S. Hartman *et al.*, 2014 Efficient marker-free recovery of custom genetic modifications with CRISPR/Cas9 in *Caenorhabditis elegans*. *Genetics* 198: 837–846.
- Berezikov, E., C. I. Bargmann, and R. H. A. Plasterk, 2004 Homologous gene targeting in *Caenorhabditis elegans* by biolistic transformation. *Nucleic Acids Res.* 32: e40.
- Chen, C., L. A. Fenk, and M. de Bono, 2013 Efficient genome editing in *Caenorhabditis elegans* by CRISPR-targeted homologous recombination. *Nucleic Acids Res.* 41: e193.
- Chiu, H., H. T. Schwartz, I. Antoshechkin, and P. W. Sternberg, 2013 Transgene-free genome editing in *Caenorhabditis elegans* using CRISPR-Cas. *Genetics* 195: 1167–1171.
- Cho, S. W., J. Lee, D. Carroll, J.-S. Kim, and J. Lee, 2013 Heritable gene knockout in *Caenorhabditis elegans* by direct injection of Cas9-sgRNA ribonucleoproteins. *Genetics* 195: 1177–1180.
- Detwiler, M. R., M. Reuben, X. Li, E. Rogers, and R. Lin, 2001 Two zinc finger proteins, OMA-1 and OMA-2, are redundantly required for oocyte maturation in *C. elegans*. *Dev. Cell* 1: 187–199.
- Dickinson, D. J., J. D. Ward, D. J. Reiner, and B. Goldstein, 2013 Engineering the *Caenorhabditis elegans* genome using Cas9-triggered homologous recombination. *Nat. Methods* 10: 1028–1034.
- Doench, J. G., E. Hartenian, D. B. Graham, Z. Tothova, M. Hegde *et al.*, 2014 Rational design of highly active sgRNAs for CRISPR-Cas9-mediated gene inactivation. *Nat. Biotechnol.* 32: 1262–1267.
- Farboud, B., and B. J. Meyer, 2015 Dramatic enhancement of genome editing by CRISPR/Cas9 through improved guide RNA design. *Genetics* 199: 959–971.
- Finney, M., and G. Ruvkun, 1990 The *unc-86* gene product couples cell lineage and cell identity in *C. elegans*. *Cell* 63: 895–905.
- Friedland, A. E., Y. B. Tzur, K. M. Esvelt, M. P. Colaiácovo, G. M. Church *et al.*, 2013 Heritable genome editing in *C. elegans* via a CRISPR-Cas9 system. *Nat. Methods* 10: 741–743.

- Frøkjær-Jensen, C., M. W. Davis, M. Ailion, and E. M. Jorgensen, 2012 Improved Mos1-mediated transgenesis in *C. elegans*. *Nat. Methods* 9: 117–118.
- Frøkjær-Jensen, C., M. W. Davis, C. E. Hopkins, B. J. Newman, J. M. Thummel *et al.*, 2008 Single-copy insertion of transgenes in *Caenorhabditis elegans*. *Nat. Genet.* 40: 1375–1383.
- Greiss, S., and J. W. Chin, 2011 Expanding the genetic code of an animal. *J. Am. Chem. Soc.* 133: 14196–14199.
- Guo, S., and K. J. Kemphues, 1996 A non-muscle myosin required for embryonic polarity in *Caenorhabditis elegans*. *Nature* 382: 455–458.
- Hajdu-Cronin, Y. M., W. J. Chen, and P. W. Sternberg, 2004 The L-type cyclin CYL-1 and the heat-shock-factor HSF-1 are required for heat-shock-induced protein expression in *Caenorhabditis elegans*. *Genetics* 168: 1937–1949.
- Hoogewijs, D., K. Houthoofd, F. Matthijssens, J. Vandesompele, and J. R. Vanfleteren, 2008 Selection and validation of a set of reliable reference genes for quantitative sod gene expression analysis in *C. elegans*. *BMC Mol. Biol.* 9: 9.
- Kamath, R. S., and J. Ahringer, 2003 Genome-wide RNAi screening in *Caenorhabditis elegans*. *Methods* 30: 313–321.
- Katic, I., and H. Großhans, 2013 Targeted heritable mutation and gene conversion by Cas9-CRISPR in *Caenorhabditis elegans*. *Genetics* 195: 1173–1176.
- Kim, H., T. Ishidate, K. S. Ghanta, M. Seth, D. Conte *et al.*, 2014 A Co-CRISPR strategy for efficient genome editing in *Caenorhabditis elegans*. *Genetics* 197: 1069–1080.
- Lee, H.-C., W. Gu, M. Shirayama, E. Youngman, D. Conte *et al.*, 2012 *C. elegans* piRNAs mediate the genome-wide surveillance of germline transcripts. *Cell* 150: 78–87.
- Leopold, L. E., B. N. Heestand, S. Seong, L. Shtessel, and S. Ahmed, 2015 Lack of pairing during meiosis triggers multigenerational transgene silencing in *Caenorhabditis elegans*. *Proc. Natl. Acad. Sci. USA* 112(20): E2667–76.
- Lo, T.-W., C. S. Pickle, S. Lin, E. J. Ralston, M. Gurling *et al.*, 2013 Heritable genome editing using TALENs and CRISPR/Cas9 to engineer precise insertions and deletions in evolutionarily diverse nematode species. *Genetics* 195: 331–348.
- Mello, C. C., J. M. Kramer, D. Stinchcomb, and V. Ambros, 1991 Efficient gene transfer in *C. elegans*: extrachromosomal maintenance and integration of transforming sequences. *EMBO J.* 10: 3959–3970.
- Munro, E., J. Nance, and J. R. Priess, 2004 Cortical flows powered by asymmetrical contraction transport PAR proteins to establish and maintain anterior-posterior polarity in the early *C. elegans* embryo. *Dev. Cell* 7: 413–424.
- Ooi, S. L., J. R. Priess, and S. Henikoff, 2006 Histone H3.3 variant dynamics in the germline of *Caenorhabditis elegans*. *PLoS Genet.* 2: e97.
- Paix, A., Y. Wang, H. E. Smith, C.-Y. S. Lee, D. Calidas *et al.*, 2014 Scalable and versatile genome editing using linear DNAs with microhomology to Cas9 Sites in *Caenorhabditis elegans*. *Genetics* 198: 1347–1356.
- Praitis, V., E. Casey, D. Collar, and J. Austin, 2001 Creation of low-copy integrated transgenic lines in *Caenorhabditis elegans*. *Genetics* 157: 1217–1226.
- Radman, I., S. Greiss, and J. W. Chin, 2013 Efficient and rapid *C. elegans* transgenesis by bombardment and hygromycin B selection. *PLoS ONE* 8: e76019.
- Sarov, M., J. I. Murray, K. Schanze, A. Pozniakovski, W. Niu *et al.*, 2012 A genome-scale resource for in vivo tag-based protein function exploration in *C. elegans*. *Cell* 150: 855–866.
- Schubert, C. M., R. Lin, C. J. de Vries, R. H. Plasterk, and J. R. Priess, 2000 MEX-5 and MEX-6 function to establish soma/germline asymmetry in early *C. elegans* embryos. *Mol. Cell* 5: 671–682.
- Shalem, O., N. E. Sanjana, E. Hartenian, X. Shi, D. A. Scott *et al.*, 2014 Genome-scale CRISPR-Cas9 knockout screening in human cells. *Science* 343: 84–87.
- Shirayama, M., M. Seth, H.-C. Lee, W. Gu, T. Ishidate *et al.*, 2012 piRNAs initiate an epigenetic memory of nonself RNA in the *C. elegans* germline. *Cell* 150: 65–77.
- Soto, M. C., H. Qadota, K. Kasuya, M. Inoue, D. Tsuboi *et al.*, 2002 The GEX-2 and GEX-3 proteins are required for tissue morphogenesis and cell migrations in *C. elegans*. *Genes Dev.* 16: 620–632.
- Srayko, M., A. Kaya, J. Stamford, and A. A. Hyman, 2005 Identification and characterization of factors required for microtubule growth and nucleation in the early *C. elegans* embryo. *Dev. Cell* 9: 223–236.
- Tenlen, J. R., J. N. Mol, N. London, B. D. Page, and J. R. Priess, 2008 MEX-5 asymmetry in one-cell *C. elegans* embryos requires PAR-4- and PAR-1-dependent phosphorylation. *Development* 135: 3665–3675.
- Tzur, Y. B., A. E. Friedland, S. Nadarajan, G. M. Church, J. A. Calarco *et al.*, 2013 Heritable custom genomic modifications in *Caenorhabditis elegans* via a CRISPR-Cas9 system. *Genetics* 195: 1181–1185.
- Waaijers, S., V. Portegijs, J. Kerver, B. B. L. G. Lemmens, M. Tijsterman *et al.*, 2013 CRISPR/Cas9-targeted mutagenesis in *Caenorhabditis elegans*. *Genetics* 195: 1187–1191.
- Wang, T., J. J. Wei, D. M. Sabatini, and E. S. Lander, 2014 Genetic screens in human cells using the CRISPR-Cas9 system. *Science* 343: 80–84.
- Ward, J. D., 2015 Rapid and precise engineering of the *Caenorhabditis elegans* genome with lethal mutation co-conversion and inactivation of NHEJ repair. *Genetics* 199: 363–377.
- Zhang, Y., D. Chen, M. A. Smith, B. Zhang, and X. Pan, 2012 Selection of reliable reference genes in *Caenorhabditis elegans* for analysis of nanotoxicity. *PLoS ONE* 7: e31849.
- Zhao, P., Z. Zhang, H. Ke, Y. Yue, and D. Xue, 2014 Oligonucleotide-based targeted gene editing in *C. elegans* via the CRISPR/Cas9 system. *Cell Res.* 24: 247–250.

Communicating editor: O. Hobert

GENETICS

Supporting Information

<http://www.genetics.org/lookup/suppl/doi:10.1534/genetics.115.178335/-/DC1>

Streamlined Genome Engineering with a Self-Excising Drug Selection Cassette

Daniel J. Dickinson, Ariel M. Pani, Jennifer K. Heppert, Christopher D. Higgins, and Bob Goldstein

Supplementary Information for:
Streamlined genome engineering with a self-excising drug selection cassette

Daniel J. Dickinson, Ariel M. Pani, Jennifer K. Heppert, Christopher D. Higgins and Bob Goldstein

Department of Biology and Lineberger Comprehensive Cancer Center
University of North Carolina at Chapel Hill
Chapel Hill, NC 27599-3280

Correspondence:
Daniel J. Dickinson
616 Fordham Hall
CB3280
Chapel Hill, NC 27599
Tel: 650-815-1923
Email: ddickins@live.unc.edu

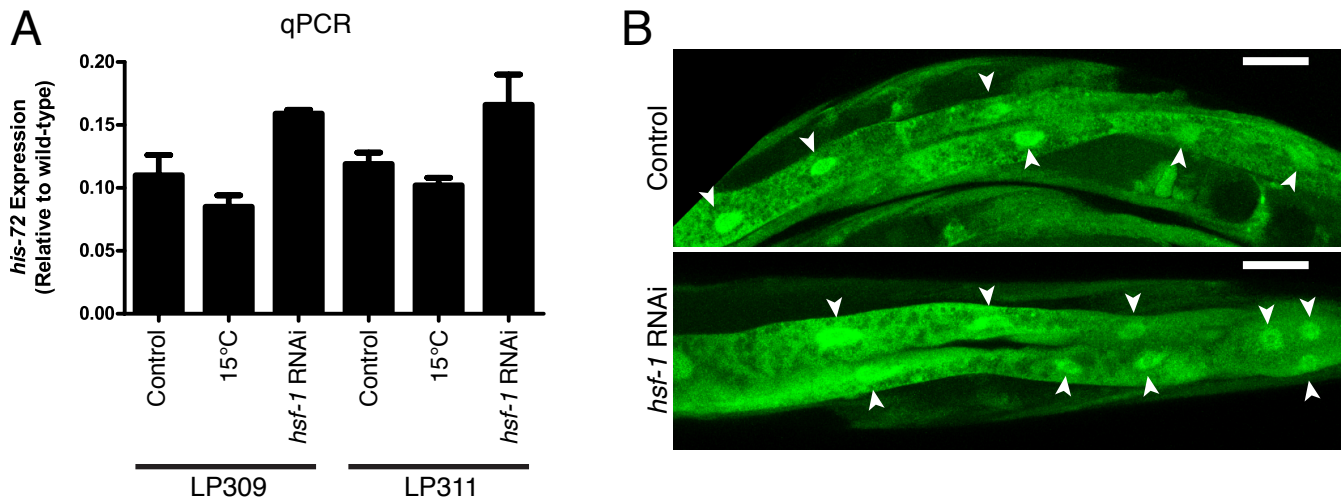


Figure S1: Spontaneous loss of SEC in intestinal cells does not require a heat shock response

A) Expression of the *his-72* ORF measured by qPCR in *mNG^{SEC}3xFlag::his-72* initial insertion strains (LP309 and LP311) following the indicated treatments. Results are the means of three replicate measurements from one experiment, and error bars indicate standard deviations.

B) mNG fluorescence in intestinal cells of *mNG^{SEC}3xFlag::his-72* animals with or without *hsf-1* RNAi. Shown are maximum intensity projections through the portion of the Z stack that includes intestinal cells. The nuclear signal is indicative of spontaneous SEC excision. Scale bars represent 20 μ m.

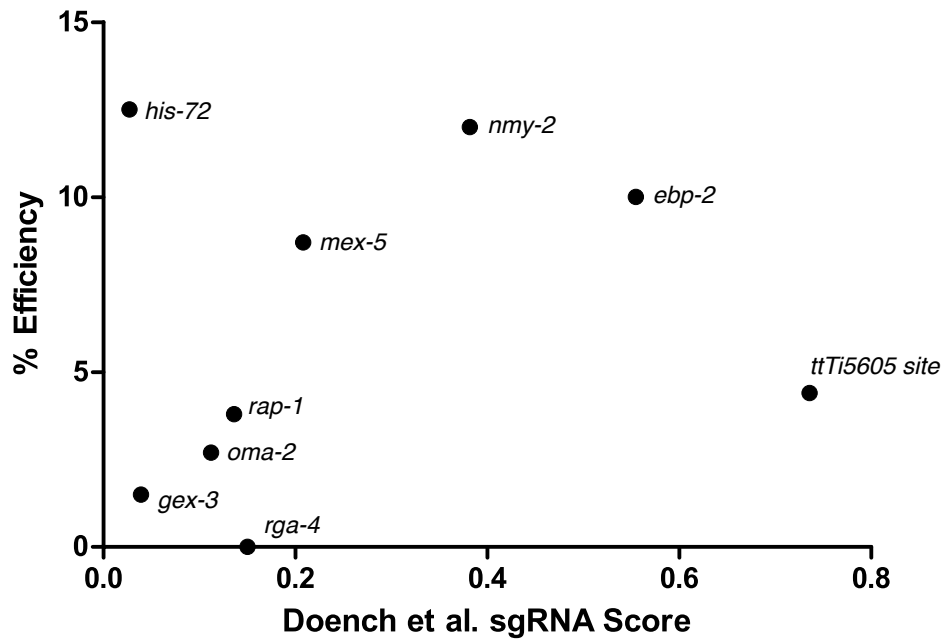


Figure S2: Relationship between sgRNA score and recombination efficiency

No statistically significant correlation between sgRNA score and recombination efficiency was observed (Spearman's $r = 0.18$; $p = 0.6$). See also Tables 1 and S2.

Table S1: Strains generated for this study

Strain Name	Genotype	Parent Strain
LP309	<i>his-72(cp73[mNG^SEC^3xFlag::his-72]) III</i>	N2
LP310	<i>his-72(cp74[mNG^3xFlag::his-72]) III</i>	LP309
LP311	<i>his-72(cp75[mNG^SEC^3xFlag::his-72]) III</i>	N2
LP312	<i>his-72(cp76[mNG^3xFlag::his-72]) III</i>	LP310
LP327	<i>his-72(cp79[mNG^SEC^3xFlag::his-72]) III</i>	N2
LP328	<i>his-72(cp80[mNG^3xFlag::his-72]) III</i>	LP327
LP329	<i>his-72(cp81[mNG^SEC^3xFlag::his-72]) III</i>	N2
LP330	<i>his-72(cp82[mNG^3xFlag::his-72]) III</i>	LP329
LP331	<i>his-72(cp83[mNG^SEC^3xFlag::his-72]) III</i>	N2
LP332	<i>his-72(cp84[mNG^3xFlag::his-72]) III</i>	LP331
LP333	<i>his-72(cp85[mNG^SEC^3xFlag::his-72]) III</i>	N2
LP334	<i>his-72(cp86[mNG^3xFlag::his-72]) III</i>	LP333
LP335	<i>his-72(cp87[mNG^SEC^3xFlag::his-72]) III</i>	N2
LP336	<i>his-72(cp88[mNG^3xFlag::his-72]) III</i>	LP335
LP337	<i>his-72(cp89[mNG^SEC^3xFlag::his-72]) III</i>	N2
LP338	<i>his-72(cp90[mNG^3xFlag::his-72]) III</i>	LP337
LP339	<i>his-72(cp91[mNG^SEC^3xFlag::his-72]) III</i>	N2
LP340	<i>his-72(cp92[mNG^3xFlag::his-72]) III</i>	LP339
LP341	<i>his-72(cp93[mNG^SEC^3xFlag::his-72]) III</i>	N2
LP342	<i>his-72(cp94[mNG^3xFlag::his-72]) III</i>	LP341
LP343	<i>his-72(cp95[mNG^SEC^3xFlag::his-72]) III</i>	N2
LP344	<i>his-72(cp96[mNG^3xFlag::his-72]) III</i>	LP343
LP323	<i>cpls59[Pmex-5::GFP::tbb-2 3'UTR + SEC] II</i>	N2
LP324	<i>cpls60[Pmex-5::GFP::tbb-2 3'UTR + SEC] II</i>	N2
LP325	<i>cpls61[Pmex-5::GFP::tbb-2 3'UTR + SEC] II</i>	N2
LP326	<i>cpls62[Pmex-5::GFP::tbb-2 3'UTR + SEC] II</i>	N2
LP345	<i>ebp-2(cp97[mNG^SEC^3xFlag::ebp-2]) II</i>	N2
LP346	<i>ebp-2(cp98[mNG^3xFlag::ebp-2]) II</i>	LP345
LP347	<i>ebp-2(cp99[mNG^SEC^3xFlag::ebp-2]) II</i>	N2
LP348	<i>ebp-2(cp100[mNG^3xFlag::ebp-2]) II</i>	LP347
LP349	<i>ebp-2(cp101[mNG^SEC^3xFlag::ebp-2]) II</i>	N2
LP350	<i>ebp-2(cp102[mNG^3xFlag::ebp-2]) II</i>	LP349
LP351	<i>ebp-2(cp103[mNG^SEC^3xFlag::ebp-2]) II</i>	N2
LP352	<i>ebp-2(cp104[mNG^3xFlag::ebp-2]) II</i>	LP351
LP353	<i>ebp-2(cp105[mNG^SEC^3xFlag::ebp-2]) II</i>	N2
LP354	<i>ebp-2(cp106[mNG^3xFlag::ebp-2]) II</i>	LP353
LP355	<i>ebp-2(cp107[mNG^SEC^3xFlag::ebp-2]) II</i>	N2
LP356	<i>ebp-2(cp108[mNG^SEC^3xFlag::ebp-2]) II</i>	N2
LP357	<i>ebp-2(cp109[mNG^3xFlag::ebp-2]) II</i>	LP356
LP358	<i>ebp-2(cp110[mNG^SEC^3xFlag::ebp-2]) II</i>	N2
LP359	<i>ebp-2(cp111[mNG^3xFlag::ebp-2]) II</i>	LP358
LP360	<i>ebp-2(cp112[mNG^SEC^3xFlag::ebp-2]) II</i>	N2
LP361	<i>gex-3(cp113[mNG^SEC^3xFlag::gex-3]) IV / nT1 [qls51] (IV;V)</i>	N2
LP362	<i>gex-3(cp114[mNG^3xFlag::gex-3]) IV</i>	LP361
LP363	<i>mex-5(cp115[mNG^SEC^3xFlag::mex-5]) / + IV</i>	N2
LP364	<i>mex-5(cp116[mNG^3xFlag::mex-5]) IV</i>	LP363
LP365	<i>mex-5(cp117[mNG^SEC^3xFlag::mex-5]) / + IV</i>	N2
LP366	<i>mex-5(cp118[mNG^SEC^3xFlag::mex-5]) / + IV</i>	N2
LP367	<i>mex-5(cp119[mNG^3xFlag::mex-5]) IV</i>	LP366
LP368	<i>mex-5(cp120[mNG^SEC^3xFlag::mex-5]) / + IV</i>	N2
LP369	<i>mex-5(cp121[mNG^3xFlag::mex-5]) IV</i>	LP368
LP370	<i>mex-5(cp122[mNG^SEC^3xFlag::mex-5]) / + IV</i>	N2
LP371	<i>mex-5(cp123[mNG^3xFlag::mex-5]) IV</i>	LP370
LP372	<i>mex-5(cp124[mNG^SEC^3xFlag::mex-5]) / + IV</i>	N2
LP373	<i>mex-5(cp125[mNG^3xFlag::mex-5]) IV</i>	LP372
LP374	<i>nmy-2(cp126[mNG^SEC^3xFlag::nmy-2]) / + I</i>	N2
LP375	<i>nmy-2(cp127[mNG^3xFlag::nmy-2]) I</i>	LP374

Strain Name	Genotype	Parent Strain
LP376	<i>nmy-2(cp128[mNG^SEC^3xFlag::nmy-2]) / +</i>	N2
LP377	<i>nmy-2(cp129[mNG^3xFlag::nmy-2])</i>	LP376
LP378	<i>nmy-2(cp130[mNG^SEC^3xFlag::nmy-2])</i> / <i>hT2 [bli-4(e937) let-(q782) qIs48]</i> (I;III)	N2
LP379	<i>nmy-2(cp131[mNG^SEC^3xFlag::nmy-2]) / +</i>	N2
LP380	<i>nmy-2(cp132[mNG^3xFlag::nmy-2])</i>	LP379
LP381	<i>nmy-2(cp133[mNG^SEC^3xFlag::nmy-2])</i> / <i>hT2 [bli-4(e937) let-(q782) qIs48]</i> (I;III)	N2
LP382	<i>nmy-2(cp134[mNG^3xFlag::nmy-2])</i>	LP381
LP383	<i>nmy-2(cp135[mNG^SEC^3xFlag::nmy-2]) / +</i>	N2
LP384	<i>nmy-2(cp136[mNG^3xFlag::nmy-2])</i>	LP383
LP385	<i>nmy-2(cp137[mNG^SEC^3xFlag::nmy-2])</i> / <i>hT2 [bli-4(e937) let-(q782) qIs48]</i> (I;III)	N2
LP386	<i>nmy-2(cp138[mNG^SEC^3xFlag::nmy-2]) / +</i>	N2
LP387	<i>nmy-2(cp139[mNG^3xFlag::nmy-2])</i>	LP386
LP388	<i>nmy-2(cp140[mNG^SEC^3xFlag::nmy-2]) / +</i>	N2
LP389	<i>nmy-2(cp141[mNG^3xFlag::nmy-2])</i>	LP388
LP390	<i>oma-2(cp142[mNG^SEC^3xFlag::oma-2])</i> V	N2
LP391	<i>oma-2(cp143[mNG^3xFlag::oma-2])</i> V	LP390
LP392	<i>oma-2(cp144[mNG^SEC^3xFlag::oma-2])</i> V	N2
LP393	<i>oma-2(cp145[mNG^3xFlag::oma-2])</i> V	LP392
LP394	<i>rap-1(cp146[mNG^SEC^3xFlag::rap-1])</i> IV	N2
LP395	<i>rap-1(cp147[mNG^3xFlag::rap-1])</i> IV	LP394
LP396	<i>rap-1(cp148[mNG^SEC^3xFlag::rap-1])</i> IV	N2
LP397	<i>rap-1(cp149[mNG^3xFlag::rap-1])</i> IV	LP396
LP398	<i>rap-1(cp150[mNG^SEC^3xFlag::rap-1])</i> IV	N2
LP399	<i>rap-1(cp151[mNG^3xFlag::rap-1])</i> IV	LP398
LP400	<i>nmy-2(cp152[mNG^3xFlag::nmy-2])</i>	LP385

Table S2: sgRNA targets used in this study
The PAM sequence is underlined.

Target	Target sequence	Doench et al. Score
Chromosome II near <i>ttTi5605</i> Mos1 insertion site	GATATCAGTCTGTTTCGTAACGG	0.736
<i>ebp-2</i> (5' end)	CGTTGACGACCATTTTGCCTCGG	0.555
<i>gex-3</i> (5' end)	GGCTTACAAAAGATGCCAGACAGG	0.039
<i>his-72</i> (5' end)	GGTACGAGCCATTGTTGTTCTGG	0.027
<i>his-72</i> (5' end; 3'GG)	TCTTGGAGCCTTTCCTCCGGTGG	0.281
<i>mex-5</i> (5' end)	GGCATCAAATAGTGCTCGTCGG	0.208
<i>mex-5</i> (5' end; 3'GG)	AATAGTGTCTCGTCGGCCGGAGG	0.427
<i>nmy-2</i> (5' end)	GATGATGTCATTATTACCGCTGG	0.382
<i>oma-2</i> (5' end)	CTGCACTACTAACGAAATAATGG	0.112
<i>oma-2</i> (5' end; 3'GG)	AGTAGTGCAGGGGAAATGGGTGG	0.392
<i>rap-1</i> (5' end)	GAGTATAAGATTGTTGTGCTCGG	0.136
<i>rap-1</i> (5' end; 3'GG)	ATTGTTGTGCTCGGATCTGGAGG	0.282
<i>rga-4</i> (5' end)	CGTTGTGTTCCATATAGTCTCGG	0.150

Supplemental Text: Detailed protocol for generating Cas9-mediated fluorescent protein knock-ins with a self-excising selection cassette (SEC)

Before the Experiment

Choose the Cas9 target site

- 1) Identify a 100-200 bp region in which the Cas9 target site should be located. We generally use a 200 bp window centered on the start codon (for N-terminal tags) or stop codon (for C-terminal tags).
- 2) Submit this genomic sequence to the Zhang lab's CRISPR design tool at <http://crispr.mit.edu>. Make sure you have selected *C. elegans* as the genome for checking specificity.
- 3) The design tool returns a list of potential targeting sequences, ranked in order of predicted specificity. We always try to choose target sites with a specificity score >95, and in most cases find a site that scores 98 or 99 (100 indicates perfect specificity). If there are several candidate sites with high specificity, choose the site that is closest to the desired insertion site (start or stop codon). The best case scenario is to have the insertion site within the guide sequence and within 10 bp of the PAM (NGG motif), so that insertion of mNG[^]SEC[^]3xFlag will disrupt the target site (Figure P1A). If this is not possible, then choose a Cas9 target sequence that is within the coding region of your gene. For the targeting sequence you choose, copy and paste the list of potential off-target sites into a Word document or Excel sheet and save this list for future reference.

Add the target sequence to the Cas9–sgRNA construct

- 1) The design tool returns target sites of the form 5' N₂₀-NGG-3', where N is any base. You need to insert the N₂₀ sequence into the Cas9–sgRNA construct (pDD162, Addgene #47549). We use NEB's Q5 Site-Directed Mutagenesis Kit to do this. Use forward primer 5' -N₂₀GTTTTAGAGCTAGAAATAGCAAGT-3', where N₂₀ is your 20 bp targeting sequence from the design tool, and reverse primer 5' -CAAGACATCTCGCAATAGG-3'.
- 2) IMPORTANT: Do not include the PAM (NGG motif) in your primers for the Cas9-sgRNA construct. The NGG motif must be present in the target DNA, but it is not part of the sgRNA.

- 3) We use sequencing primer 5' -GGTGTGAAATACCGCACAGA-3' to verify correct insertion of the targeting sequence.

Design primers to add homology arms to an FP-SEC vector

Figure 1C shows our strategy for cloning homology arms into FP-SEC vectors. Homology arms are generated by PCR and inserted in place of the *ccdB* negative selection markers, which are flanked by restriction sites. We chose these particular restriction sites so that no residual sequence is left behind after addition of the homology arms. *ccdB* negative selection makes this cloning strategy exceptionally robust and efficient: in a pilot experiment, we generated 8 repair templates in parallel in a single afternoon. 7/8 of these reactions yielded >80% correct clones; the remaining reaction also yielded correct clones, albeit at a lower frequency.

You need to design four primers: two for each homology arm. These primers will amplify the homology arms and add sequence overlaps for Gibson assembly to the ends of each arm. If FP::SEC insertion will not disrupt the Cas9 target site, your primers will also need to introduce silent mutations to prevent Cas9 from cutting the repair template.

You have a choice of two possible pairs of restriction enzymes to digest the FP-SEC vector: AvrII+SpeI or ClaI+SpeI. If AvrII and SpeI are used, the repair template will include a flexible linker between the 5' homology arm and FP (this is useful for generating C-terminal tags). If ClaI and SpeI are used, the 5' homology arm will be fused directly to the FP, with no added sequence (this is useful for N-terminal tags, or when no flexible linker is desired). Figure P1 shows sample primer designs for each situation.

Detailed primer design instructions:

- 1) First, decide whether additional mutations are needed to prevent Cas9 from cutting the repair template. We make additional mutations whenever the insertion site is not within the 10 bp of the target sequence closest to the PAM. Additional mutations are made using synonymous codons so that the amino acid sequence is not altered (See Figure P1B for an example). If possible, the simplest and most effective approach is to mutate the PAM (NGG motif), since this motif is absolutely required for cleavage of a substrate by Cas9. If a PAM mutation is not feasible, introduce as many mutations as possible (at least 5-6) in the target sequence.

- 2) Each homology arm should be 500-700 bp long. The positions of the two primers most proximal to the FP^{SEC}3xFlag module (i.e., the reverse primer for the 5' homology arm and the forward primer for the 3' homology arm) are fixed by the need to insert FP^{SEC}3xFlag at a specific location. The positions of the distal primers are more flexible. We design the proximal primers first based on our desired insertion site, and then use Primer-BLAST to pick the best possible distal primers.
- 3) Decide with FP you want to insert, and consult Table P1 for the sequence that needs to be added to the end of each primer to allow Gibson assembly.
- 4) Ideally, the primer length should be less than 60 bp, because longer primers are much more expensive and fail more often. If you find you need a longer primer because your Cas9 target site is far away from the insertion site, it might be more cost effective to purchase a synthetic DNA fragment (we like IDT's gBlocks) containing the homology arm instead of using PCR.
- 5) Before ordering primers, double check that the mNG::3xFlag will be in frame with your gene of interest.

Add homology arms to the repair template

- 1) Prepare the vector:
 - Grow bacteria carrying the FP-SEC vector and miniprep the plasmid DNA. Note that, prior to replacing the *ccdB* elements with homology arms, FP-SEC vectors must be grown in cells that are resistant to *ccdB* (*ccdB* Survival cells).
 - Digest an entire miniprep of FP-SEC vector overnight at 37°C (consult Table P1 for which construct and enzymes to use).
 - Purify the digested vector using a PCR cleanup spin column to remove the enzymes. Process the entire digested vector as one sample; do not attempt to gel purify individual bands.
 - The digested, purified vector may be stored at 4°C for at least a few months and re-used to construct multiple repair templates.
- 2) Prepare the homology arms:
 - Generate two PCR products (the homology arms) using genomic DNA as the template and the primers you designed above.
 - Mix the two PCR products and purify them together on a single PCR cleanup spin column.

N-terminal mNeonGreen::3xFlag	
<i>Digest vector pDD268 with Clal and SpeI</i>	
5' arm forward primer:	5'-acgttgtaaaacgacggccagtcgccggca-(Homology arm sequence)-3'
5' arm reverse primer:	5'-CATGTTGCTCTCTCCCTTGGAGACCAT-(Cas9 target mutations)-(Homology arm sequence)-3'
3' arm forward primer:	5'-CGTGATTACAAGGATGACGATGACAAGAGA-(Cas9 target mutations)-(Homology arm sequence)-3'
3' arm reverse primer:	5'-tcacacaggaacagctatgaccatgttat-(Homology arm sequence)-3'
C-terminal mNeonGreen::3xFlag (with flexible linker)	
<i>Digest vector pDD268 with AvrII and SpeI</i>	
5' arm forward primer:	5'-acgttgtaaaacgacggccagtcgccggca-(Homology arm sequence)-3'
5' arm reverse primer:	5'-CATCGATGCTCTGAGGCTCCCGATGCTCC-(Cas9 target mutations)-(Homology arm sequence)-3'
3' arm forward primer:	5'-CGTGATTACAAGGATGACGATGACAAGAGA-(Cas9 target mutations)-(Homology arm sequence)-3'
3' arm reverse primer:	5'-ggaaacagctatgaccatgttatcgatttc-(Homology arm sequence)-3'
N-terminal GFP::3xFlag	
<i>Digest vector pDD282 with Clal and SpeI</i>	
5' arm forward primer:	5'-acgttgtaaaacgacggccagtcgccggca-(Homology arm sequence)-3'
5' arm reverse primer:	5'-TCCAGTGAACAATTCTTCTCTTTACTCAT-(Cas9 target mutations)-(Homology arm sequence)-3'
3' arm forward primer:	5'-CGTGATTACAAGGATGACGATGACAAGAGA-(Cas9 target mutations)-(Homology arm sequence)-3'
3' arm reverse primer:	5'-tcacacaggaacagctatgaccatgttat-(Homology arm sequence)-3'
C-terminal GFP::3xFlag (with flexible linker)	
<i>Digest vector pDD282 with AvrII and SpeI</i>	
5' arm forward primer:	5'-acgttgtaaaacgacggccagtcgccggca-(Homology arm sequence)-3'
5' arm reverse primer:	5'-CATCGATGCTCTGAGGCTCCCGATGCTCC-(Cas9 target mutations)-(Homology arm sequence)-3'
3' arm forward primer:	5'-CGTGATTACAAGGATGACGATGACAAGAGA-(Cas9 target mutations)-(Homology arm sequence)-3'
3' arm reverse primer:	5'-ggaaacagctatgaccatgttatcgatttc-(Homology arm sequence)-3'
N-terminal YPET::3xFlag	
<i>Digest vector pDD283 with Clal and SpeI</i>	
5' arm forward primer:	5'-acgttgtaaaacgacggccagtcgccggca-(Homology arm sequence)-3'
5' arm reverse primer:	5'-TCCTGTAATAACTTCTCTTTTACAT-(Cas9 target mutations)-(Homology arm sequence)-3'
3' arm forward primer:	5'-CGTGATTACAAGGATGACGATGACAAGAGA-(Cas9 target mutations)-(Homology arm sequence)-3'
3' arm reverse primer:	5'-tcacacaggaacagctatgaccatgttat-(Homology arm sequence)-3'
C-terminal YPET::3xFlag (with flexible linker)	
<i>Digest vector pDD283 with AvrII and SpeI</i>	
5' arm forward primer:	5'-acgttgtaaaacgacggccagtcgccggca-(Homology arm sequence)-3'
5' arm reverse primer:	5'-CATCGATGCTCTGAGGCTCCCGATGCTCC-(Cas9 target mutations)-(Homology arm sequence)-3'
3' arm forward primer:	5'-CGTGATTACAAGGATGACGATGACAAGAGA-(Cas9 target mutations)-(Homology arm sequence)-3'
3' arm reverse primer:	5'-ggaaacagctatgaccatgttatcgatttc-(Homology arm sequence)-3'
N-terminal TagRFP-T::3xFlag	
<i>Digest vector pDD284 with Clal and SpeI</i>	
5' arm forward primer:	5'-acgttgtaaaacgacggccagtcgccggca-(Homology arm sequence)-3'
5' arm reverse primer:	5'-CTTGATGAGCTCTCTCCCTTGGAGACCAT-(Cas9 target mutations)-(Homology arm sequence)-3'
3' arm forward primer:	5'-CGTGATTACAAGGATGACGATGACAAGAGA-(Cas9 target mutations)-(Homology arm sequence)-3'
3' arm reverse primer:	5'-tcacacaggaacagctatgaccatgttat-(Homology arm sequence)-3'
C-terminal TagRFP-T::3xFlag (with flexible linker)	
<i>Digest vector pDD284 with AvrII and SpeI</i>	
5' arm forward primer:	5'-acgttgtaaaacgacggccagtcgccggca-(Homology arm sequence)-3'
5' arm reverse primer:	5'-CATCGATGCTCTGAGGCTCCCGATGCTCC-(Cas9 target mutations)-(Homology arm sequence)-3'
3' arm forward primer:	5'-CGTGATTACAAGGATGACGATGACAAGAGA-(Cas9 target mutations)-(Homology arm sequence)-3'
3' arm reverse primer:	5'-ggaaacagctatgaccatgttatcgatttc-(Homology arm sequence)-3'
N-terminal mKate2::3xFlag	
<i>Digest vector pDD285 with Clal and SpeI</i>	
5' arm forward primer:	5'-acgttgtaaaacgacggccagtcgccggca-(Homology arm sequence)-3'
5' arm reverse primer:	5'-CATGTTTTCTTTAATGAGCTCGGAGACCAT-(Cas9 target mutations)-(Homology arm sequence)-3'
3' arm forward primer:	5'-CGTGATTACAAGGATGACGATGACAAGAGA-(Cas9 target mutations)-(Homology arm sequence)-3'
3' arm reverse primer:	5'-tcacacaggaacagctatgaccatgttat-(Homology arm sequence)-3'
C-terminal mKate2::3xFlag (with flexible linker)	
<i>Digest vector pDD285 with AvrII and SpeI</i>	
5' arm forward primer:	5'-acgttgtaaaacgacggccagtcgccggca-(Homology arm sequence)-3'
5' arm reverse primer:	5'-CATCGATGCTCTGAGGCTCCCGATGCTCC-(Cas9 target mutations)-(Homology arm sequence)-3'
3' arm forward primer:	5'-CGTGATTACAAGGATGACGATGACAAGAGA-(Cas9 target mutations)-(Homology arm sequence)-3'
3' arm reverse primer:	5'-ggaaacagctatgaccatgttatcgatttc-(Homology arm sequence)-3'

Table P1: Primers for insertion of homology arms into FP::SEC vectors.

- 3) Mix 1 μL of vector, 4 μL of homology arms and 5 μL of isothermal assembly enzyme mix (we use NEBuilder HiFi DNA assembly mix from NEB). Incubate 1h @ 50°C or as directed by the enzyme manufacturer. Transform 2 μL of the reaction to suitable competent cells.
- 4) Isolate DNA from 3-6 clones and sequence with M13 Forward and Reverse primers to verify correct insertion of the homology arms. This cloning procedure is efficient enough that screening clones prior to sequencing is not necessary.

Injections to Generate Knock-ins

Day 0: Injection

- 1) Prepare an injection mix containing the following:
 - 10 ng/ μL homologous repair template
 - 50 ng/ μL Cas9-sgRNA construct with your targeting sequence
 - Fluorescent co-injection markers (to label extrachromosomal arrays):
 - 10 ng/ μL pGH8 (Prab-3::mCherry neuronal co-injection marker; Addgene #19359)
 - 5 ng/ μL pCFJ104 (Pmyo-3::mCherry body wall muscle co-injection marker; Addgene #19328)
 - 2.5 ng/ μL pCFJ90 (Pmyo-2::mCherry pharyngeal co-injection marker; Addgene #19327)

Prepare plasmid DNA using Invitrogen's PureLink mini-prep kit, which gives high injection efficiencies.

- 2) Inject the mixture into the gonads of 50-60 young adult worms of strain N2 (or substitute any strain you like).
- 3) Transfer the injected worms to new seeded plates (three animals per plate works well in our hands). Use regular NGM plates (no drug) at this stage. Also make a control plate with un-injected worms, so that when you do the drug selection it can serve as a negative control.
- 4) Put the plates at 25°C and let the worms lay eggs without selection for 2-3 days.

Day 2 or 3: Add hygromycin

Prepare and filter sterilize a 5 mg/mL hygromycin solution in water. For 6 cm plates poured with 10 mL agar plates, pipet 500 μL of drug onto the surface of each plate of worms, for a final concentration of ~ 250 $\mu\text{g}/\text{mL}$ (if using different size plates, adjust the volume accordingly). Swirl gently so that the solution covers the entire surface of the plate, then let it dry. Put the worms back at 25°C. Note: In our hands, it does not make any difference whether we add the drug on

the second or third day after injection, but the drug must be added no later than the third day in order to kill untransformed F1 progeny before they reproduce and overcrowd the plates.

Day 6 or 7: Pick initial knock-in worms

- 1) Examine the plates and identify those that contain Roller (Rol) animals that survived the hygromycin treatment. Knock-in plates should be obvious: there should be lots of animals, they should look totally healthy, and L3 and older worms should be Rol (the Rol phenotype is not expressed in L1 or L2 larvae). Do not waste your time picking from plates that have only a few, sick-looking worms.
- 2) Candidate knock-in animals are L4/adults that 1) survive hygromycin selection; 2) are Rol; and 3) lack the red fluorescent extrachromosomal array markers. Note that we occasionally see a plate with many wild-type worms that survived selection, but do not pick these – they typically carry extrachromosomal arrays or rearrangements. Also note that, in our experience, rare non-fluorescent animals on plates with lots of mCherry(+) animals (i.e., lots of array animals) are usually false positives.
- 3) Single 5-10 candidate knock-in adults to new plates without hygromycin.

If you do not see any candidate knock-ins at this stage, or if you have fewer lines than you'd like, wait 3 days and then examine the plates again. We sometimes find knock-ins 9-10 days after injection (when the F3 are young adults) that were missed during the first round of screening.

Day 9 or 10: Look for homozygous plates

Look for plates where 100% of L4s and adults are Rollers. These are homozygous knock-in animals. They can be maintained indefinitely, outcrossed if desired, or mated to another genetic background. The strong Rol phenotype makes it very easy to follow the knock-in in crosses (but note that Rol males mate poorly). You can also take L1s from these plates and proceed directly to heat shock to remove the selectable markers.

It is straightforward to generate lethal mutations with our strategy, because knock-in alleles can be isolated and maintained as heterozygotes. You will know that your knock-in is lethal if you see only heterozygous plates (i.e., plates with ~1/4 wild-type worms and 1/4 dead embryos). You should expect your initial knock-in to be lethal if you are making an N-terminal tag on an essential gene, because the initial knock-in is a transcriptional null mutation.

Note: It is impossible to tell whether two strains that originated from the same injection plate derive from independent insertion events or a single insertion event. Therefore, although we single 5-10 worms from each plate in the previous step, we keep only one line from each plate.

Selectable marker removal

Figure P2 shows the overall scheme for selectable marker removal. In most cases, the initial knock-in is homozygous viable and marker removal is extremely simple (Figure P2A).

If the initial knock-in is lethal, marker removal is slightly more complicated because heterozygous knock-in animals segregate wild-type animals at each generation, which makes it impossible to identify animals that have excised the marker based on wild-type phenotype alone (Figure P2). In this situation, there are two choices. If your knock-in strain is visibly fluorescent, you can simply heat shock heterozygotes and identify animals that have excised the marker based on a wild-type phenotype plus visible fluorescence (Figure P2B). If fluorescence in your knock-in strain is too dim to see by eye, you need to mate in a GFP-marked balancer chromosome first (Figure P2C). Mate males carrying an appropriate GFP-marked balancer to Rol knock-in hermaphrodites. Pick GFP-positive, Rol animals from the F1 progeny. These animals should now no longer segregate wild-type progeny in the absence of heat shock (Figure P2C). Use these balanced knock-in worms for subsequent steps.

Day 0: Heat shock

- 1) Pick 6-8 L1/L2 larvae to each of three new plates. It is possible to perform marker excision using older animals, but using young larvae results in the highest efficiency because the germ cells have not yet begun to divide.
- 2) Heat shock the plates at 34°C for 4 hours (or at 32°C for 4-5 hours) in an air incubator to activate expression of *hs::Cre*. After heat shock, return the plates to 20°C or 25°C.

Day 5-7: Pick knock-in animals that have lost the marker

Pick wild-type worms to new plates. The animals you will pick will be the F1 progeny of the L1/L2 larvae that you heat shocked in the previous step. Be careful not to pick these animals too early, since the Rol phenotype conferred by *sqt-1(d)* does not appear until L3. To be safe, we only pick L4 and adult animals at this step.

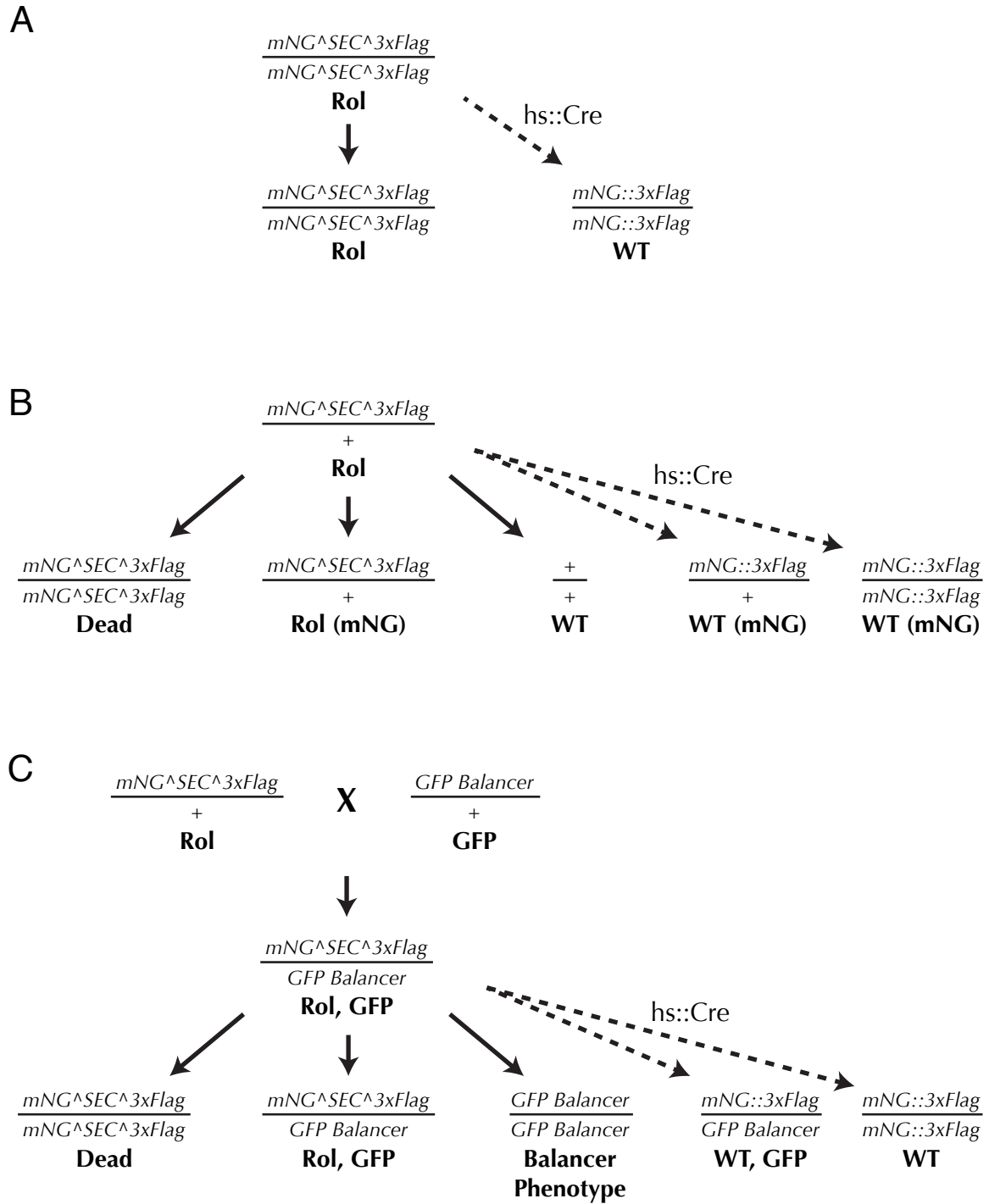


Figure P2: Genetic schemes for marker self-excision. (A) For homozygous viable knock-ins, the situation is simple: after heat shock, any wild-type worms will have lost both copies of SEC. (B) If the knock-in is homozygous lethal, the strain produces 1/4 wild-type progeny at each generation. This makes it impossible to unambiguously identify worms that have lost SEC based on wild-type phenotype alone, although knock-ins may be identifiable if they show visible fluorescence. (C) A simple, 1-step cross to introduce a GFP balancer chromosome results in a strain that does not segregate any wild-type progeny. Heat shock-induced marker excision in this background generates wild-type animals that can be easily and unambiguously identified.

Movie S1: Plate phenotype of *sqt-1(d)* animals before and after marker excision

The left panel shows animals homozygous for a single-copy insertion of a *sqt-1(d)::hygR* selectable marker; L3 and older worms exhibit a strong and highly penetrant Roller phenotype . The right panel shows the same strain after marker excision; wild-type animals are easily recognizable.

Available for download as an AVI file at

www.genetics.org/lookup/suppl/doi:10.1534/genetics.115.178335/- /DC1